Project Number: ME-JB3-DCP1

Development of a Plasma Source with Integrated Particulate Injector and Charging Sensor

A Major Qualifying Project Report

Submitted to the Faculty

of

WORCESTER POLYTECHNIC INSTITUTE

in partial fulfillment of the requirements for the

Degree of Bachelor of Science

in Mechanical Engineering

by

Joseph Basile

McConnell Dickson

William Flaherty

Brian Kolk

Date: March 3, 2007

Approved:

Prof. John Blandino, Major Advisor

Executive Summary

The goal of this MQP was to design, build, and test a chamber for creating and probing dusty plasmas. This was actually two distinct problems. First, the chamber had to be designed to create a plasma environment. Second, a mechanism needed to be developed that would dispense dust in a controlled fashion into the plasma. Due to their functional similarities, the initial design was based on an electron bombardment ion thruster discharge chamber using a thermionic filament cathode.

The chamber was designed to meet certain design requirements. Because the team had little practical machining knowledge it needed to be designed for ease of machining. Also, it had to be designed to mount inside an existing vacuum chamber in Higgins Labs room 016. The final design was very similar in shape to other ion sources, consisting of an 8 in tall, 8 in diameter cylinder. The gas is injected into the cap of the chamber, from where it diffuses into the discharge chamber. A suspended filament cathode is used to ionize this gas and create the plasma. Rare earth magnets are also used to apply a Lorentz force to the electrons to increase their residence time in the gas and hence the number of ionizing collisions. The dust is also injected through a hole in the chamber's cap. It then free falls through the discharge chamber and is charged through collisions with ions and electrons. At the bottom of the chamber, some of these dust particles fall into a diagnostic sensor (the Charge Detection Mass Spectrometer) that will measure their charge. Also, a Langmuir probe is used to collect data on the plasma to investigate its properties.

Almost all the manufacturing was done by the team. Simple parts were created using the various manual machines (such as mills and lathes) available in the Higgins Shops. More complicated parts were made using the Computer Numerically Controlled (CNC) machines. None of the team members had any practical machining knowledge before the start of this MQP. All training was done through short introductory courses and hands on experience in the shop. Though there were some minor problems due to the team's inexperience, all the parts needed to create the discharge chamber were created successfully.

Over the three terms of the project, the team successfully researched, designed, and built the dusty plasma chamber and most of the Langmuir probe and CDMS diagnostics. Unfortunately, due to a mechanical problem with the vacuum equipment, the team did not get to test it. The team hopes to continue working on the experiment on a time-permitting, no-credit basis during the last academic term of 2008. It is expected that the hardware will be used by undergraduate and graduate students in the future as well.

Table of Contents

List of Figures

List of Tables

1. Introduction

Development of a Plasma Source with Integrated Particulate Injector and Charging Sensor, advised by Professor Blandino is a Major Qualifying Project whose purpose is to design, build, and test an apparatus to investigate particulate charging in a plasma. The study also sought to investigate the sensitivity of charging to various plasma parameters.

One of the applications of this study is to improve the understanding of different spacecraft environments. The phenomena of particulate charging in a plasma is also relevant to magnetically confined plasmas for power generation and materials processing. Understanding how a dusty plasma interacts with sensitive satellite equipment is critical in prolonging satellite life as well as understanding how it could possibly affect the data being gathered.

The study involved designing an apparatus which will allow the dropping of micron sized particles into an argon plasma. This results in the charging of the particles and is intended to simulate a plasma environment one might encounter near a spacecraft in low earth orbit or in a plasma processing facility. The sensors that will be measuring the plasma are the charge detection mass spectrometer (CDMS) and a plasma probe. The CDMS will measure the charge of the particles being dropped through the argon plasma, whereas the plasma probe system will measure the electron temperature as well as the ion density.

Due to the conceptual similarity of the "dusty plasma chamber" to an electron bombardment ion thruster (a kind of electric propulsion), there is much previous research on discharge chamber size and magnet placement among other optimization factors to assist in the

construction of the apparatus. Research from those areas was used to understand rules of thumb to simplify the design of this complicated apparatus. It also allowed the team to focus on building and gathering data instead of generating design criteria which are already established in the field of electric propulsion. The conceptual sketch of the discharge chamber can be seen in Figure 1.

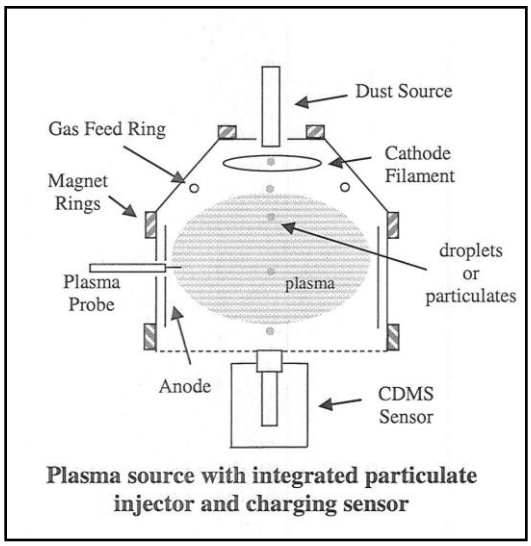

Figure 1: Preliminary Discharge Chamber Design

When the apparatus is constructed and functioning, the collected data will provide insight on plasma processes, and particulate charging. Experiments will also help determine if the CDMS can be used to measure the charge of solid particles; it has been exclusively used for the charge of liquid droplets in electrospray experiments. This apparatus will also support Professor Gatsonis' research, which will bridge his computational modeling of the dusty plasma with actual experimental data. Our apparatus will provide the experimental data.

2. Prior Work

When studying plasma interaction with charged dust particles, it is critical to understand the physics of magnet placement around the discharge chamber. Since ion propulsion shares many characteristics with our dust charging study, it was useful to find literature that provided insight to the design of the particular type of plasma source used in both electric propulsion and this experiment. There were also rules of thumb that could be used for our particular study.

Bennet, Ogunjobi, and Menart from the Wright State University in Ohio published a paper titled *Computational Study of the Effects of Cathode Placement, Electron Energy, and Magnetic Field Strength on the Confinement of Electrons.* This work investigated how permanent magnets in a ring-cusp configuration can keep electrons from being lost to the discharge chamber. They did not study the electron energy or the magnetic strength. However, they did examine the cathode placement magnet orientation, and the number of magnets through computational methods [1].

The paper reports that as a general rule of thumb, "the magnetic circuit should be designed such that the largest gauss field line is closed." It goes on to suggest that closing the largest gauss contour is best done though computational modeling, What the paper means is that though all field lines are closed, the magnetic field strength needs to be strong enough to contain the electrons sufficiently in the discharge chamber to maximize the ionization of the argon gas. Since there are many different variables that dictate the shape of the magnetic field lines, the computational modeling helps assess the relative importance of factors like the anode size, the strength of magnets needed, and magnet thickness which dictates the shape of the magnetic field lines. The thicker the magnets, the straighter the magnetic field lines. [1].

There are also issues with the magnetic field having holes, or places in where the field intensity is low enough that the electrons can reach the anode before they have collided a sufficient number of times with neutral argon atoms. This is caused by the magnets being too far apart. This issue can be solved by doing proper computational models and having a sufficiently sized anode. So, to summarize, it is required to have the largest gauss field line contained within the anode, and it's also necessary to understand how the distance of the magnets affect the shape of the magnetic field.

To determine how well they were implementing the rules-of-thumb, the authors used two programs: PRIMA and MAXWELL 2D. PRIMA is a computer program that uses the Monte Carlo method to simulate motion of particles in a domain through a magnetic field that the programmer defines. The model results are within about 20% of the experimental results [1].

On the other hand, MAXWELL 2D calculates the magnetic field produced by the ring magnets. MAXWELL 2D uses Maxwell's equations and computes the magnetic fields. It will take a mesh and will iterate until the result converges. Bennet et al. used MAXWELL 2D for data to input into PRIMA to come with a more accurate representation of the magnetic field and how it influences the electrons [1].

The Write State paper also reports on a study of where to place the cathode. The authors found that the position of the cathode had little to do with the ability of the magnetic field to confine the ions. Two figures from the Wright State paper, are shown in Figure 2 below. These are plots of confinement length vs. cathode position. Confinement length is defined as the distance that the electron travels during its lifetime. One can see that the lines are horizontal; this is how the authors concluded that the confinement length and cathode position do not depend

upon each other. They did not indicate any specific conditions where these are dependent upon each other.

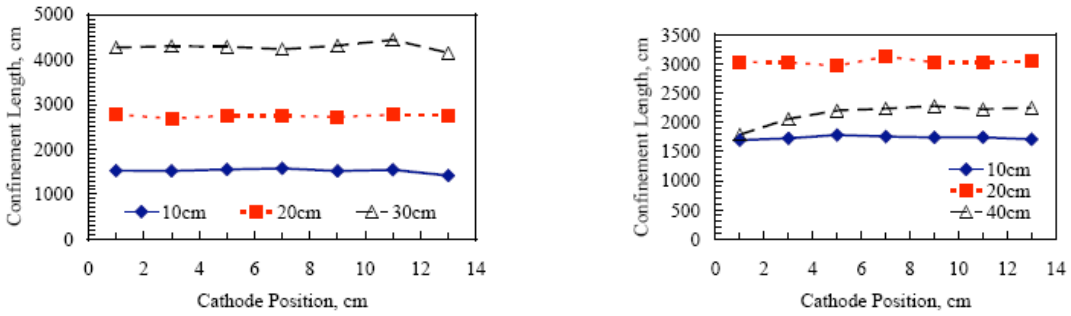

Figure 2: Cathode Position vs. Confinement Length [1]

Another parameter that was investigated was the magnetic field strength. It was found that the thickness of the magnet as well as its location on the discharge chamber controls the field strength distribution. In addition, the number of magnets affects the confinement length, which is indicative of how well the magnetic field contains the electrons within the chamber. Generally, the number of magnets increases as the confinement length decreases. For smaller confinement lengths the field is less able to contain electrons. As more magnets are introduced to the system, more cusps develop which increase the probability of an electron to escape the magnetic field. The paper recommends that it is best to have two rings of magnets instead of three because the third adds another cusp in the magnetic field for the electrons to hit the discharge chamber. This would reduce the overall apparatus efficiency [1].

3. Background

3.1 Electricity and Magnetism

This section provides a brief review of some basic relationships in electricity and magnetism that will be used in the project. Coulomb's law describes the resultant force of two charged particles. Two particles having charges q_1 and q_2 are separated by distance r and the electrostatic force is equal to

$$F = \frac{k(|q_1||q_2|)}{r^2} \quad \text{(Eq. 1)}$$

k is the electrostatic constant, $8.988 \cdot 10^9 \ \mathrm{N} \cdot \frac{\mathrm{m}^2}{\mathrm{C}^2}$ [2]. If the two charged particles have similar charges, i.e. both are positively or both are negatively charged, then they exert a repulsive force. If they have opposite charges, one negatively charged and one positively charged, then there is an attractive force. Any charge (*q*), either positive or negative can be written as

$$\mathrm{q} = \eta \cdot \mathrm{e} \quad \text{(Eq. 2)}$$

N is an integer and *e* is the elementary charge, $e = 1.602 \cdot 10^{-19}$ C, the smallest possible unit of charge [2]. The electron and proton both have a charge equal to the elementary charge in magnitude.

Charged particles with similar charge behave like a gas that would try to spread out in a container. Excess charged particles will uniformly spread over the surface of a spherical conductor. This arrangement that occurs allows for maximum distance between all like charged particles on the spherical surface. If the surface of a spherical conductor is negatively charged, then any incoming negatively charged particle will be repulsed as if the charge on the sphere

were concentrated in the center of the sphere. Similarly, if the surface is positively charged, then any incoming positively charged particle will be repulsed.

A magnetic field is a field that exerts a force on moving electric charges. For example, a magnetic field occurs with current in a wire, this is an electromagnet. Permanent magnets have a magnetic field from the collective arrangement of electrons in a material. The magnetic force on a charged particle moving through a magnetic field is written as

$$F_b = q(\mathbf{v} \times \mathbf{B}) \quad (\text{Eq. } 3)$$

Where *q* is the charge of the particle; ***v*** is the vector velocity; ***B*** is the vector magnetic field. The force acting on this charged particle is always perpendicular to both the velocity direction and the magnetic field direction, thus resulting in a helical spin of the charged particle. This effect can be seen in Figure 3.

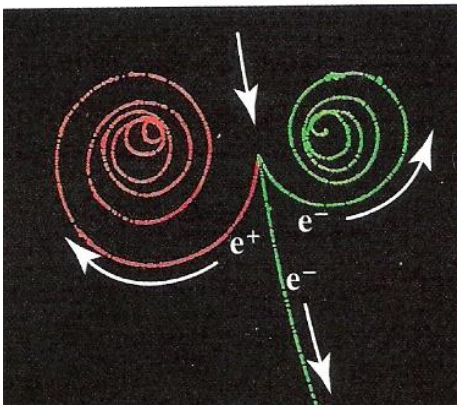

Figure 3: Helical Path of an Electron/Positron in a Uniform Magnetic Field [2]

The strength of magnetic fields or magnets can be represented by magnetic field lines. A stronger magnetic field is represented by a higher density of magnetic field lines in that area.

The SI unit for magnetic fields is the Tesla (T). A magnetic field strength normally refers to flux density which is Tesla. Magnetic flux, Φ_m, is the integral of the magnetic field over an area with units of Weber.

$$1\mathrm{T} = \frac{\text{Newton}}{\text{coulomb} \cdot \left(\frac{\text{meter}}{\text{second}}\right)} \quad (\text{Eq. } 4)$$

$$\Phi_m = \iint B \cdot dS \quad (\text{Eq. } 5)$$

Some examples of the strength of magnetic fields are: at the surface of a neutron star which has strength of 10^8 T, at the earth's surface is 10^{-4} T, and a refrigerator magnet is 0.1 T [2].

3.2 Plasmas

Plasmas can form under high temperatures when the molecules in a given gas begin to dissociate (break apart) and form ions and free electrons. A plasma has been defined as a, "quasi-neutral gas of charged and neutral particles which exhibits collective behavior." In order for the plasma to be considered quasi-neutral, it must have a collective net charge close to zero, but it must also allow for local charge concentrations and other electromagnetic effects. Because the atoms in plasmas can have electrons in excited (high energy) states, plasma can emit visible light. Plasmas are also effective conductors of electrical energy because they contain free electrons and ions. [3]

2.1 Temperature of Plasmas

An interesting topic in the study of plasmas is the concept of temperature. The temperature of a given gas is determined by the average translational speed of the particles constituting such a gas. Because gases generally contain particles moving at every possible

velocity, a histogram of all particle velocities will follow a Gaussian distribution pattern. That is, they will fall under a standard bell curve. This equilibrium distribution is called a Maxwellian velocity distribution. This velocity distribution is a function of the temperature of the given gas. The average kinetic energy of a gas is defined as:

$$E_{av} = \frac{1}{2}kT \quad \text{(Eq. 6)}$$

Where *k* is Boltzmann's constant, $k = 1.38x10^{-23}\frac{J}{K}$ and T is the temperature of the gas. [3]

In plasmas, this relationship can become more complex. Because ions and free electrons are dissociated in plasma, they can have different velocity distributions and thus, different temperatures. It is not unusual for laboratory controlled plasmas to reach temperatures of 1,000,000 K, but because typical densities are so low, the total heat energy within the plasma is actually quite low and heating of equipment by plasma is generally not a serious concern.

2.2 Debye Shielding

A characteristic exhibited by plasmas that must be taken into account is the shielding of electric fields due to the distribution of highly mobile, free electrons. If an object of a given potential is placed in a plasma, the object will attract particles of opposite charge and repel particles with the same charge. That is, a positively charged object will attract electrons while a negatively charged object will repel electrons, leaving a deficit or surplus of ions, relative to the number of electrons, in the local vicinity of the charged object. This results in a layer of charged particles, called a sheath, to form around sources of electric fields. The charges of the particles in the sheath effectively cancel out the electric field created by the charged object. The thickness (radius) of the sheath in the order of a characteristic length λ_D is called the Debye length and is defined as:

$$\lambda_D = \sqrt{\frac{\epsilon_0 k T_e}{n \cdot e^2}} \quad \text{(Eq. 7)}$$

Where ε_0 is the permittivity of free space, T_e is the electron temperature, n is the number density of electrons (electrons per cubic meter), and e is the elementary charge (e = 1.602x10^{-19} C). In order for a gas to be considered a plasma, the Debye Length must be much smaller than the overall size of the plasma. This is usually dependant on the plasma having sufficient overall density.

Furthermore, the number of charged particles within the Debye Length can be computed using the number density of the particles in question:

$$N_D = \left(\frac{4\pi}{3}\right) n(\lambda_D)^3 \quad \text{(Eq. 8)}$$

This is also called the plasma parameter. [3]

2.3 Plasma Frequency

The Plasma Frequency is the frequency of periodic oscillations of the local number density of electrons within a plasma. The Plasma Frequency ω_p is defined as:

$$\left(\omega_p\right)^2 = \frac{ne^2}{\epsilon_0 m} \quad \text{(Eq. 9)}$$

Where m=9.11x10^{-31} kg, the mass of an electron. Inverting the Plasma Frequency ω_p results in the plasma period τ. Experiments involving plasmas should be conducted so that the process or phenomenon under investigation spans periods of time exceeding that of the plasma period. If the period of time under which the plasma is observed is shorter than the plasma period, the

observed average number density of electrons in the plasma will differ significantly from the actual average number density of electrons in the plasma. In summation, a plasma is only recognizable as a plasma over periods of time exceeding the plasma period [4].

3.3 Dusty Plasmas

A dusty plasma is plasma which contains charged micron or sub-micron sized particulates. They are prevalent in space as seen in the zodiacal light, the Orion Nebula and the tail of a comet. Based upon spectroscopy data, the dust grains in these clouds are dielectrics and metallic such as ice silicates, graphite, magnetite and amorphous carbons [5]. Natural dusty plasmas contain particles of various sizes while artificially generated dusty plasmas tend to contain particles of a specified size.

In our solar system, sources of dust are lunar ejecta, space debris, micrometeoroids and the asteroid belt [5]. Collisions of comets and asteroids release between 0.25 tonnes s^{-1} and 20 tonnes s^{-1} of dusty gas in the solar system. The dust will spiral into the sun, due to solar wind drag and Poynting-Robertson light drag. This is a loss of orbital angular momentum by gyrating particles associated with their absorption and re-emission of the solar radiation [5]. It will take between thousands and millions of years for particles smaller than 1cm to reach the sun. The National Aeronautics and Space Administration (NASA) is able to collect samples of this dust using high-altitude aircraft at an altitude of between 18 and 20 km.

When there is no external disturbance present a dusty plasma is macroscopically neutral. There will be no net resulting electric charge when the dusty plasma is in equilibrium.

$$q_i \cdot n_{io} = e \cdot n_{eo} - q_d \cdot n_{do} \quad (\text{Eq. } 10)$$

Where q_i is the ion charge, n_{i0} is the number density of ions, e is the electron charge, n_{e0} is the number density of electrons, q_d is the dust particle charge and n_{d0} is the number density of dust particles.

Some of the differences between a plasma and a dusty plasma can be seen in Table 1.

The basic differences between electron–ion and dusty plasmas.

Characteristics	Electron–ion plasma	Dusty plasma
Quasi-neutrality condition	$n_{e0} = Z_i n_{i0}$	$Z_d n_{d0} + n_{e0} = Z_i n_{i0}$
Massive particle charge	$q_i = Z_i e$	$\|q_d\| = Z_d e \gg q_i$
Charge dynamics	q_i = constant	$\partial q_d / \partial t$ = net current
Massive particle mass	m_i	$m_d \gg m_i$
Plasma frequency	ω_{pi}	$\omega_{pd} \ll \omega_{pi}$
Debye radius	λ_{De}	$\lambda_{Di} \ll \lambda_{De}$
Particle size	uniform	dust size distribution
$E \times B_0$ particle drift	ion drift at low B_0	dust drift at high B_0
Linear waves	IAW, LHW, etc	DIAW, DAW, etc
Nonlinear effects	IA solitons/shocks	DA/DIA solitons/shocks
Interaction	repulsive only	attractive between grains
Crystallization	no crystallization	dust crystallization
Phase transition	no phase transition	phase transition

Table 1: Differences between Plasma and Dusty Plasma [5]

The table shows that the dust grain charge-mass ratio (q_d/m_d) has some distribution. The dusty plasma also modifies low-frequency waves such as ion-acoustic waves (IAW) and creates new ones like dust acoustic waves (DAW) and dust ion-acoustic shocks (DIA).

A property of a dusty plasma is its macroscopic neutrality. If the dusty plasma is locally disturbed from its equilibrium position, the internal space charged field gives rise to collective particle motions inside the plasma which tend to restore the original charge neutrality. The

inertia of the particles will cause an overshoot of the equilibrium position and oscillate around the equilibrium position. The frequency of the motion of these particles is known as the plasma frequency.

$$w_{ps} = \sqrt{\frac{4\pi n_s q_s^2}{m_s}} \quad \text{(Eq. 11)}$$

Where *s* is either the charge of electrons, ions, or dust particles. This differs from the frequency for a plasma, equation 9.

Another important characteristic of a dusty plasma is the frequency associated with collision of electrons, ions, and dust particles with stationary neutrals.

$$\nu_{sn} = \eta_n \sigma_s^n V_{ts} \quad \text{(Eq. 12)}$$

Where η_n is neutral number density, σ_s^n σ_s^n is the scattering cross section, $V_{ts} = \sqrt{\frac{K_b T_s}{m_s}}$ which is the thermal speed and *s* = *e,i,d* for electrons, ions, dust particles respectively. The collisions of plasma particles with the stationary neutrals will dampen their collective oscillations. Oscillations will be damped when the collision frequency ν_{sn} is smaller than the plasma frequency ω_p.

The Coulomb coupling parameter is what determines the possibility of the formation of dusty plasma crystals. The Coulomb coupling parameter is

$$\Gamma_c = \left(\frac{Z_d^2 e^2}{a k_b T_d}\right) \exp\left(-\frac{a}{\lambda_d}\right) \quad \text{(Eq. 13)}$$

$k_b T_d$ is the dust thermal energy, a is the distance between two like charged dust particles, Z_d is the number of charges on the dust particle. The dusty plasma is weakly coupled when $\Gamma_c << 1$, and is strongly coupled when $\Gamma_c >> 1$. When the dust grains are massive, the plasma is strongly coupled because of the large number of charges on the dust, low temperatures and small intergrain distance [5].

Dusty plasmas created in laboratories are different than astrophysical dusty plasmas. Laboratory discharges have geometric boundaries whose structure, composition, temperature, conductivity influence the formation of the dust grains. Also, in laboratory dusty plasmas, the external circuit, which is required to ionize the gas, imposes varying boundary conditions.

There are different methods to create dusty plasma in laboratories. For example, in the work by Fortov, *et al*, in 1997, a dusty plasma device can make dusty plasma by surface ionization of potassium atoms on a hot tantalum plate and a dust dispenser dropping particles down into the plasma [5]. The dusty plasma device can be seen in Figure 4.

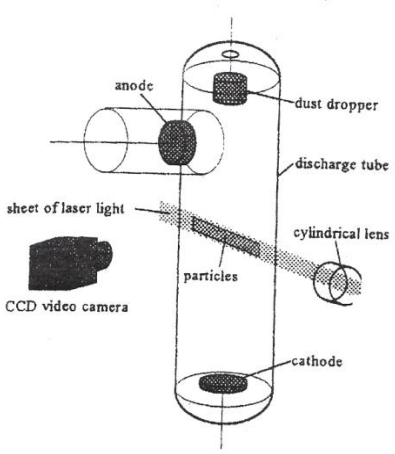

Figure 4: Dusty Plasma Device [5]

Other examples of non-stellar dusty plasmas are plasmas in fusion devices which are contaminated by dust which is heavier than hydrogen isotopes. The dust comes from sputtering, evaporation and sublimation of wall material at extremely high temperatures. Also, solid-fuel combustion produces dusty plasma as exhaust with the dust being Al_2O_3 for aluminum-coated solid fuel and MgO for magnesium-coated solid fuel.

3.4 Diagnostics

Two diagnostics will be used to collect data in the experiment. The first is the Charge Detection Mass Spectrometer (CDMS). Its main purpose will be to record the charge and velocity of the dust grains after having passed through the plasma. The second will be a Langmuir probe. This probe will collect data regarding the state of the plasma.

The CDMS used in this work was first designed for use in colloid thruster research conducted by Professor John Blandino. It is constructed of three main parts: the retarding screen, the charge detection tube, and the collection cup. The original intent of the CDMS was to investigate charged droplets, and therefore the function of the CDMS will be explained by following the path of a drop through the device. As the drop first enters the CDMS it passes through a screen. The CDMS is designed so that the screen may be charged to high voltages. The purpose of this is to create a retarding curve for the droplets. This is accomplished by increasing the voltage on the screen in steps and subsequently measuring the number of droplets that come through over a set time period. When the number of droplets is close to zero it has reached the stopping potential of the droplets, measured in volts. This number plays an important part in the final calculations after data collection is complete. This step is done separately from droplet charge detection, and the voltage applied to the screen is turned off before the collection of droplets.

After traveling past the retarding screen, the droplet enters the charge detection tube. As the droplet passes through the detection tube it induces a charge on the tube. This imprint is then passed through an amplifier and then into an oscilloscope. Figure 5 shows a waveform created by a droplet passing through the charge detection tube.

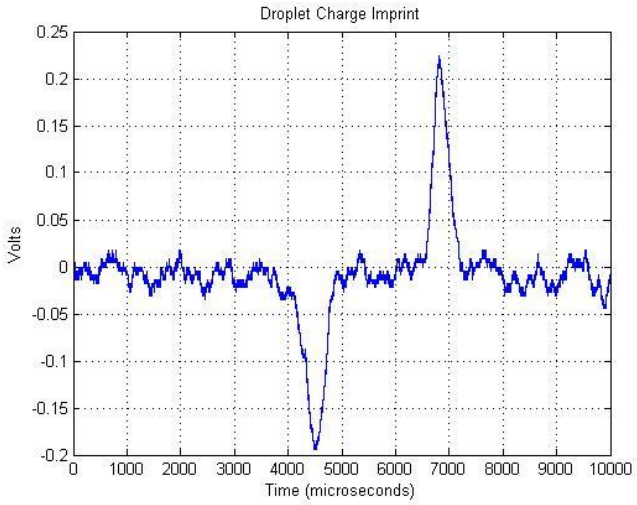

Figure 5: Droplet Waveform

The x-axis represents time steps, and the y-axis shows voltage from the amplifier. The first peak can be taken as indicating the moment the droplet entered the tube, and the second peak can be taken as the time the droplet exits the tube. Using these two points it is possible to determine the time-of-flight of the droplet through the tube of known length. Determining the charge of the droplet is slightly more complicated. By integrating Ohm's Law the charge of the droplet can be found by taking half of the integral of the voltage signal divided by the grounding resistance. Care must be taken to make sure the sign of the charge is correct. In the calculation the charge will always be a positive number, but this is only because of the sign convention used. If the fluid (or dust particle) is negatively charged, then the final charge must be multiplied by negative one to get the correct number. Finally, after leaving the charge detection tube, the droplet

terminates into a grounded cup that is electrically isolated from all the other parts in the CDMS. This is done to ensure that there is no charge buildup in the device. Such a buildup would result in erroneous data being collected.

Data acquisition with the CDMS is accomplished by passing the induced charge, of the tube caused by the droplet signal, through an amplifier and then to an oscilloscope. The oscilloscope is then connected to a computer through a DAQ card. The data is written to a file through a LabView Virtual Instrument (VI). Two separate VI's are used to collect data. The first is used to collect the retarding potential data, and also has controls for the power supplies used to charge the retarding screen. The other VI captures the droplet waveforms as shown in Figure 5 which are used to calculate the induced charge. This data is written to a LabView measurement file, which can then be imported into Matlab. For each droplet a measurement file is created consisting of 10,000 data points. The time step between points is controllable via the oscilloscope, and is most often set at 10^{-4} seconds per step.

Once the data is in the LabView measurement file format it can be loaded into Matlab using multiple M-Files that were developed specifically for the task. Using these M-Files, it is possible to analyze hundreds of droplets in only a few minutes.

The CDMS used in this project is the second generation of the probe. The original CDMS was designed by Professor John Blandino and a group of undergraduate students at WPI in collaboration with Dr. Manuel Gamero-Castaño at NASA's Jet Propulsion Laboratory. A cross section of the old CDMS can be seen in Figure 6.

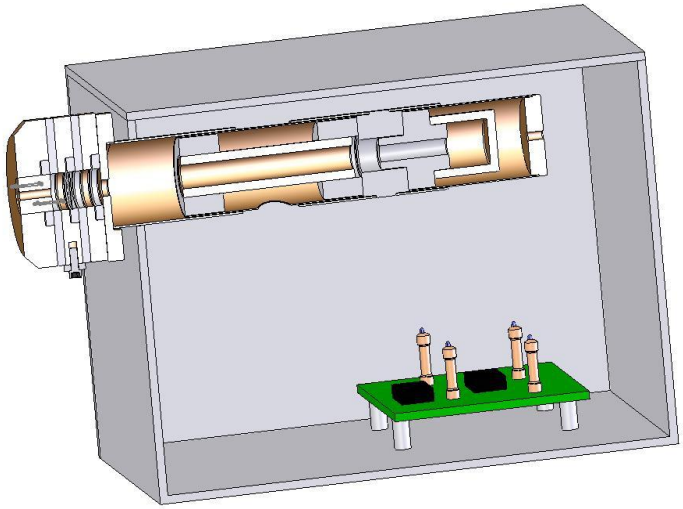

Figure 6: Original CDMS

The main design considerations were only that it be able to mount to the test apparatus to be used in Professor Blandino's droplet fission project. In the spring of 2007 it was decided that a second generation of the CDMS should be designed and built. The main goal was to reduce the cross section of the CDMS so that it could be more easily used in other applications, such as in the exhaust plume of a colloid thruster. The overall design goals were to develop something cylindrical, self-contained, easily assembled/disassembled, and with the ability to be mounted in several different applications. The resulting sensor is made up of a series of concentric discs that are held together with two structural rods made from 4-40 threaded rod. All connections are done through miniature coax connections through the back of the probe, resulting in a perfectly circular cross section. A cut away of the new CDMS can be seen in Figure 7.

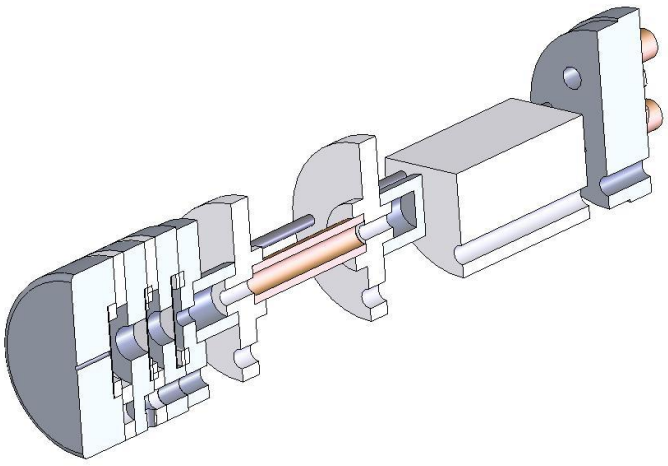

Figure 7: Cutaway of second generation CDMS

The second probe used in this experiment is a Langmuir probe. This type of probe consists of, at its most basic level, a wire. One end of this wire is bare and exposed to the plasma environment. The other end is shielded, passed outside the vacuum chamber, and then connected to a current-voltage source such as a source meter (e.g. Keithley 2410). This source meter is used to sweep a range of voltages through the wire, and the resulting current induced in the wire is measured. This current is induced by the incident flux of electrons and ions (depending on the bias voltage of the wire). By using the current information obtained by the probe, the ion and electron densities of the plasma can be obtained. A typical voltage versus current graph is shown in Figure 8.

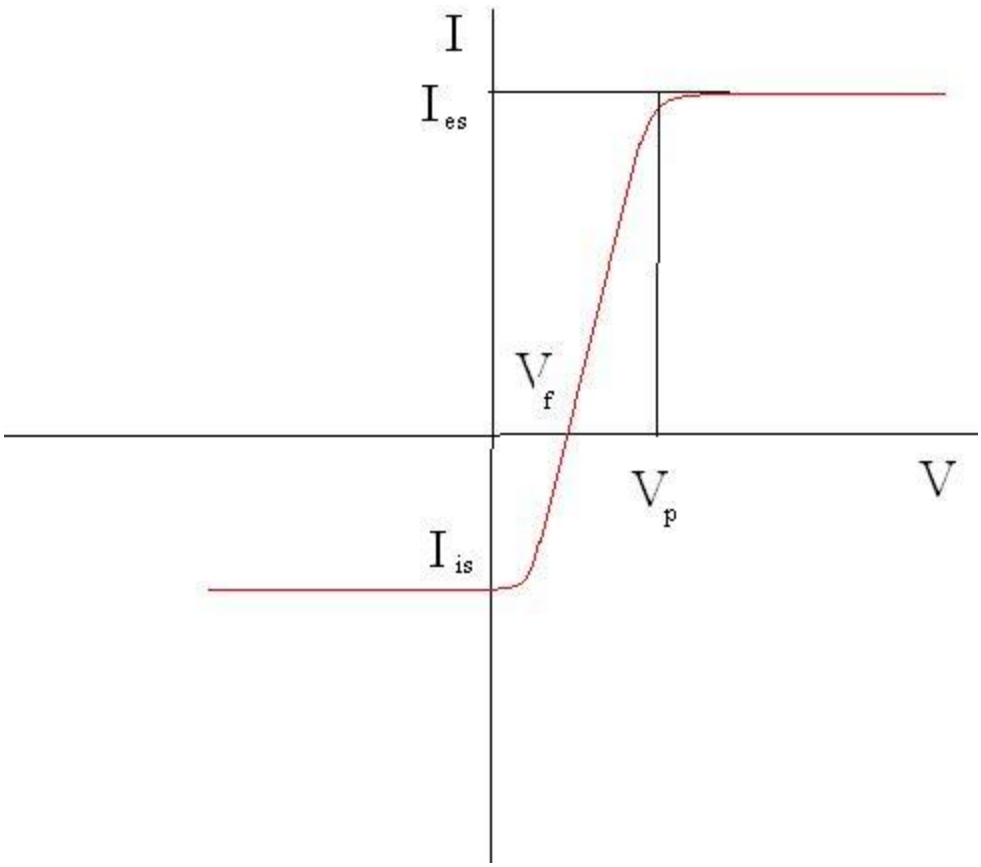

Figure 8: Sketch of Current vs. Voltage Curve

At point V_p indicated in Figure 8, the plasma is at the same potential as the probe. Points I_{es} and I_{is} are the electron and ion saturation currents, respectively. The saturation current is the point where the flux of that particular species has reached the maximum value the plasma can sustain, regardless of the bias voltage. The final point of interest on this graph is V_f, where the curve crosses the x-axis. This point is known as the floating potential of the plasma, and is the point at which the probe will draw equal electron and ion current. This is also the potential that the probe would have if it was electrically isolated from ground [6].

As discussed earlier in this report, any charged or grounded surface within a plasma will develop a sheath around it. The Langmuir probe is not immune to this effect. The simplest sheath

geometry to consider would be a flat plate with large area. Alternatively, a very thin sheath on a curved surface might also be considered planar on a local scale. Unfortunately, there are few applications here an extremely large plate can be worked into the system design. Also, this type of probe would have the possibility of having far more effect on the plasma than something small would. Though the analysis is decidedly more difficult, a thin wire probe as described in the beginning of this section is the most commonly used due to its small size. The analysis of these wire probes, though more difficult, has been done many times before, and the equations necessary are readily available. The equation is derived using the conservation of energy and momentum of a charged particle in cylindrical coordinates. After much manipulation the resulting expression for the collected current is given by:

$$I = 2en_s ad\sqrt{\left(\frac{2e\left|\Phi_p - V_B\right|}{m}\right)} \quad \text{(Eq. 14)}$$

Where I is the ion saturation current, e is the electron charge, n_s is the plasma density, a is the probe radius, d is the probe length, $\left|\Phi_p - V_B\right|$ is the potential difference between the probe and the plasma, and m is the electron mass. It should be noted that the term inside the square root is an estimation of electron velocity at the probe surface due to the accelerating force created by the potential difference. After measuring the saturation currents with the Langmuir probe, there is still one unknown, the plasma potential. This is determined using the current versus probe voltage graph that is created during the source meter sweep, shown in Figure 8. The top "knee" of the graph, where the electron current saturates, occurs at a potential which corresponds to the plasma potential. After determining this all variables are known in the equation. It should be noted that by "plasma density" one is not referring to the amount of gas in the chamber. Rather, it is the density of either electrons or ions in the plasma (which are equal in a "quasineutral"

plasma) depending on which saturation current is used. With this information it is possible to determine the density of the plasma produced. For example, should the ion density be extremely low it is obvious that the gas is very weakly ionized [6]. For this experiment a simple wire Langmuir probe will be used to collect the information, and then the data will be analyzed using either the aforementioned equation, or another more appropriate to the plasma regime anticipated (thin sheath, orbit motion limited etc.) This will allow data to be gathered on what, if any, effect the dust has on the plasma.

3.5 Vacuum Technology

The fundamentals of vacuum technology are important to understanding this MQP. The term "vacuum" is generally used when there is low gas density and hence low pressure. There are a few classifications of vacuums. A low Vacuum is from atmosphere to 25 torr, a medium vacuum is from 25 to 10^{-3} torr, a high vacuum is from 10^{-3} to 10^{-9} torr, and an ultra high vacuum is anything lower than 10^{-9} torr. The MQP will be operating at roughly in the 10^{-7} torr range. Since it is easier to create plasmas in a low pressure environment, this projects' discharge chamber will be located inside of a larger vacuum chamber. To accomplish this, the team will utilize a vacuum pump, which can extract gas from a sealed chamber and expel it to the atmosphere. To give a perspective on the relationship between density and the number of particles, a chamber at 1 mtorr (.133 Pa) will have approximately air $3.5x10^{13}$ cm^3 particles.

3.5.1 Ionization Gages

The ionization gage measures the pressure inside a vacuum chamber, while under a vacuum. Ion gages measure the pressure by a having a glowing tungsten or thoria-coated iridium filament emit electrons. This occurs when the filament reaches a temperature of 1800° C. The

cathode emits electrons which impact and ionize the neutral gas in the vacuum. The ionized gas then the positive ion current is measured by an electrometer. The ion current across the filament is linearly proportional to the pressure in the chamber. [10].

When the pressure gets down to 10^{-3} torr, common methods of measuring pressure instruments, such as using a hydrostatic gauge, cannot be used. However, ionization gages are useful when measuring pressures from the 10^{-3} to 10^{-10} torr. Using an ion gage in an environment higher than 10^{-3} torr will cause the filament to burn out. For this experiment the team will be using one of these devices to measure the pressure in the vacuum chamber since we will be in the 10^{-3} to 10^{-10} torr range. Using a mechanical gauge is possible from atmosphere to about 1 torr [10].

Different gasses will affect the pressure reading due to atomic weight. For example, having a container with helium will increase the reading that the ionization gives by 6.8 times that of air. An important parameter of an ion gauge is its sensitivity factor. If an ionization calibrated for air is reading 10^{-4} torr when there is helium inside, then actual pressure would be 6.8×10^{-4} torr.

3.5.2 Roots Blower

The roots blower is a type of displacement pump which is designed for maximum pumping efficiency at pressures from 1 to 10^{-3} torr. Its basic components include two rotating rotors mounted on twin shafts. As these rotate, the pump creates a pressure differential drawing the air out of the chamber and into a backing pump. It is not uncommon for the rotors to reach a speed up to 3,000 rpm with a clearance of a few thousandths of an inch between the two rotors. It is important to know that it's rare for a vacuum system to use only a roots blower for achieving

a high vacuum Often pumps are used in series to accommodate their pressure range requirements. For example, for the vacuum setup for this dusty plasma MQP, a piston pump operates from atmosphere down to about 7 torr, and then a roots blower starts at 7 torr down to 10^{-3} torr [10].

3.5.3 Turbomolecular Pump

These pumps are a highly effective and are quick at pumping down a chamber. The pump has a turbine which is similar in concept to what some turbocharged cars use. Though our experiment doesn't utilize these kinds of pumps, it's worth mentioning them as a viable option of achieving a high vacuum.

The rotors inside the pump can spin anywhere from 20,000 rpm to 90,000 rpm depending upon the size of the pump. The speed of the turbine blades are determined by making the edge of the blades nearly equal to the speed at which the molecular velocities of the gas which increases the probability that the gas will be removed from the container. Adequately sized turbo pumps can reach pressures on the order of 10^{-10} torr, but most reach a terminal pressure in the 10^{-7} torr range.

The blades are designed in such a way as to redirect gas molecules in the direction of the exhaust. An advantage to using this pump is it doesn't contaminate the chamber with any liquids or gasses originating from the pump. The turbine blades are often suspended in a magnetic bearing which makes the vacuum even cleaner since no lubrication is ever needed. However, since these pumps have such small tolerances care is needed to make sure that no foreign object enters the pump. With proper care, these pumps can operate with average use for one to three years without needing any maintenance.

To use this pump one needs a roughing pump, such as the rotary pump. This is because if the turbomolecular pump started at atmosphere, the load on the pump would be too great. When the roughing pump cannot take the pressure down any further, one would then start the turbo pump and continue pumping down the chamber.

3.5.4 Vapor Diffusion Pump

The diffusion pump is often used as an alternative to a turbomolecular pump. Though it is cheaper than the turbo pump, it runs the risk of contaminating the chamber with oil that the diffusion pump uses. The pump works by creating a jet of oil or mercury vapor which pushes a gas to the bottom of the pump which then is taken out of the exhaust through a pipe called a foreline and then through another mechanical pump (often referred to as a roughing pump). There is a momentum transfer between the oil or mercury vapor and the gas. At the bottom of the diffusion pump, there is a heater that boils the oil or mercury vapor and directs it back up through the jet spray ports. This process repeats and ultimately pumps down a chamber. The sides of the pump chamber are water cooled so that the fluid vapor condenses and falls back into the reservoir which increases the efficiency of the pumping system.

The molecular weight of the gas affects how effective the pump is going to be. For example, the pump would have to run more oil per second to adequately pump light gasses than for heavier gasses. It is not uncommon for a diffusion pump to run about 4 L/s for air, but that number is dependent on the specific needs of the experiment and the size of the chamber.

Diffusion pumps also need to maintain a certain pressure in their foreline. When the foreline pressure hits a critical pressure, the pump stalls and the working fluid is then pumped in reverse into the vacuum chamber causing oil backflow into the chamber. This can be detrimental

and typically requires the entire chamber to be cleaned. Forelines are typically kept at a pressure below 50 mtorr.

3.5.5 Cryopump

The project group will be using a Cryopump to pump the chamber from 10^{-3} torr to about 10^{-10} torr. This is a unique pump that condenses gas on a cold surface. This then effectively lowers the pressure in the vacuum chamber. However, there are certain operational restrictions, such as it can only be started from the millitorr range. This pump also only works on certain gasses. This is because all gasses have different freezing and boiling points, and the gas might not condense on the cool surface of the pump if it can't get cold enough to condense the gas. This design issue was met by creating certain cryopumps that have multiple cold surfaces. There are outer stages which condense the gasses with the highest boiling point, then the inner stages address the gasses with lower boiling points, such as nitrogen. Below is a picture of a cross section of a cryopump; the 10 grey fins are the cold surfaces [10].

Often cryopumps are cooled by liquid nitrogen; some also have other methods of keeping cool, such as a cryocooler. Many cryopumps also use liquid helium which can get down to 4 Kelvin instead of liquid nitrogen, which can get down to 77 Kelvin. Using the liquid helium makes the pump much more effective since the cold plate can condense gasses more effectively [10].

4. Design and Fabrication

4.1 Conceptualization and Design Requirements

The original design for the discharge chamber was based on a 15cm ion engine. A picture of the original design concept can be seen in Figure 9.

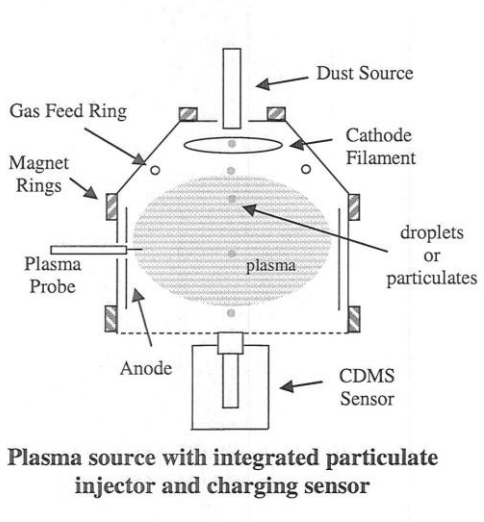

Figure 9: Original Plasma Source Design

The main differences between the plasma source and an ion engine were the dust source, cathode, gas supply, and the absence of an accelerating screen. In order to investigate the charging of dust as it falls through plasma it was necessary to add a dust source to the basic ion engine discharge chamber design. To achieve the most uniform charging of the dust the dispenser was designed to allow the dust to fall along the central axis of the discharge chamber. In an ion engine the cathode is typically be a hollow cathode, where as this design utilized a thermionic filament cathode in order to minimize cost. A typical ion engine utilizes a gas flow through the hollow cathode as well as a separate gas supply, this project required a single gas

supply. Also, the screen and accelerating grids, a prominent feature on an ion engine, were omitted from this design since there was no need to accelerate the particles and generate force.

The first change to this design was the realization that the WPI machine shops worked solely in English units, and therefore all the chamber dimensions would have to be converted. This required major dimensions to be altered so they would be in whole numbers. The second major change was to eliminate the conical top of the discharge chamber and replace it with a flat cap. The team made this decision based on the complexity of machining required to make a conical top. It was also decided to modify the magnet design. Due to the cost of rare earth magnets the team decided to approximate magnet rings with a series of small cube magnets arranged in a circle.

After these modifications were made the team was able to break the discharge chamber into different parts to be designed. These parts were the top cap (with integrated gas feed and cathode), the main chamber, the anode, the gas outlet mesh assembly (including the holder for the CDMS probe), the magnets, and the particulate injector.

4.2 Discharge Chamber and Components

The discharge chamber comprises the bulk of the device and houses all of the plasma source components. It consists of an 8 in (outer diameter) aluminum tube with a wall thickness of .125 in, a top cover, and a 0.125 in thick mesh to allow for free flow of argon gas out of the bottom of the chamber.

The top cover has an integrated gas feed system allowing controlled argon flow into the chamber. To ionize the argon, an electrical system utilizing a cathode mounted below the gas feed ring and an anode sheet encircling the area intended to house the plasma was used (see

section 4.2.1). The purpose of the electrical system was to create an electrical current through the argon, resulting in collisions between free flowing electrons and argon atoms. These collisions cause electrons to be stripped from the argon atoms, ionizing them. The end result is free electrons, ions, and neutral gas atoms: a partially ionized plasma.

To maximize the likelihood of these collisions, the electrons in the chamber were forced to follow helical trajectories resulting from a magnetic field. The magnetic field was create by samarium-cobalt magnets placed inside the chamber. One ring of six 0.5 in cube magnets was place on the underside of the cap, while another ring was mounted on the inside of the chambers outer wall, just below the anode. A simulation was used to determine the optimal number, location, and orientation of these magnets. Budgetary concerns were also factored into the selection process for the magnets. The mesh mounted at the bottom of the chamber was designed to allow the escape of argon from the chamber and as a mounting point for the CDMS.

To integrate the discharge chamber into the vacuum apparatus, a set of two extruded aluminum H-frames was constructed, as shown in Figure 10. This system was also used to support the Langmuir probe and its control assembly.

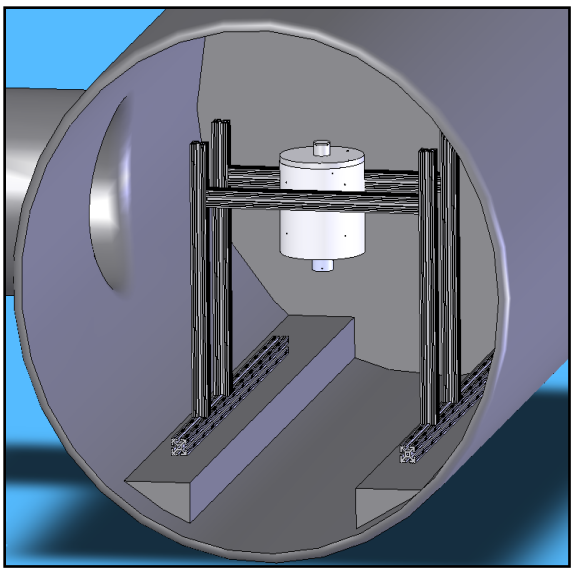

Figure 10: Discharge Chamber Mount

4.2.1 Electrical Components

In the earliest design phase, the electrical systems in the chamber were composed of a tungsten filament cathode mounted to the underside of the chambers' top cover with ceramic standoffs and a positively biased aluminum sheet wrapped along the inside of the chamber wall and electrically isolated with ceramic standoffs. This basic setup was maintained throughout each iteration of the design process, but the specifications changed significantly over time.

The electrical system is designed to produce a current flowing from the negatively biased cathode ring at the top of the chamber to the positively biased anode along the inner wall as shown in Figure 11.

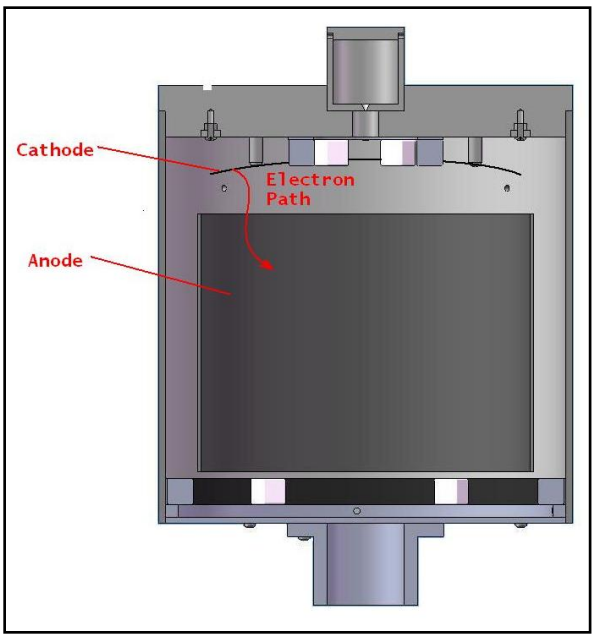

Figure 11: Electron Path Through Discharge

Argon gas is injected into the discharge chamber and ionized as the atoms are struck by the free flowing electrons. The excess electrons then terminate on the anode.

Figure 12 shows an early design iteration of these components, with the cathode out of view. SolidWorks 2007 was used to accurately model these components.

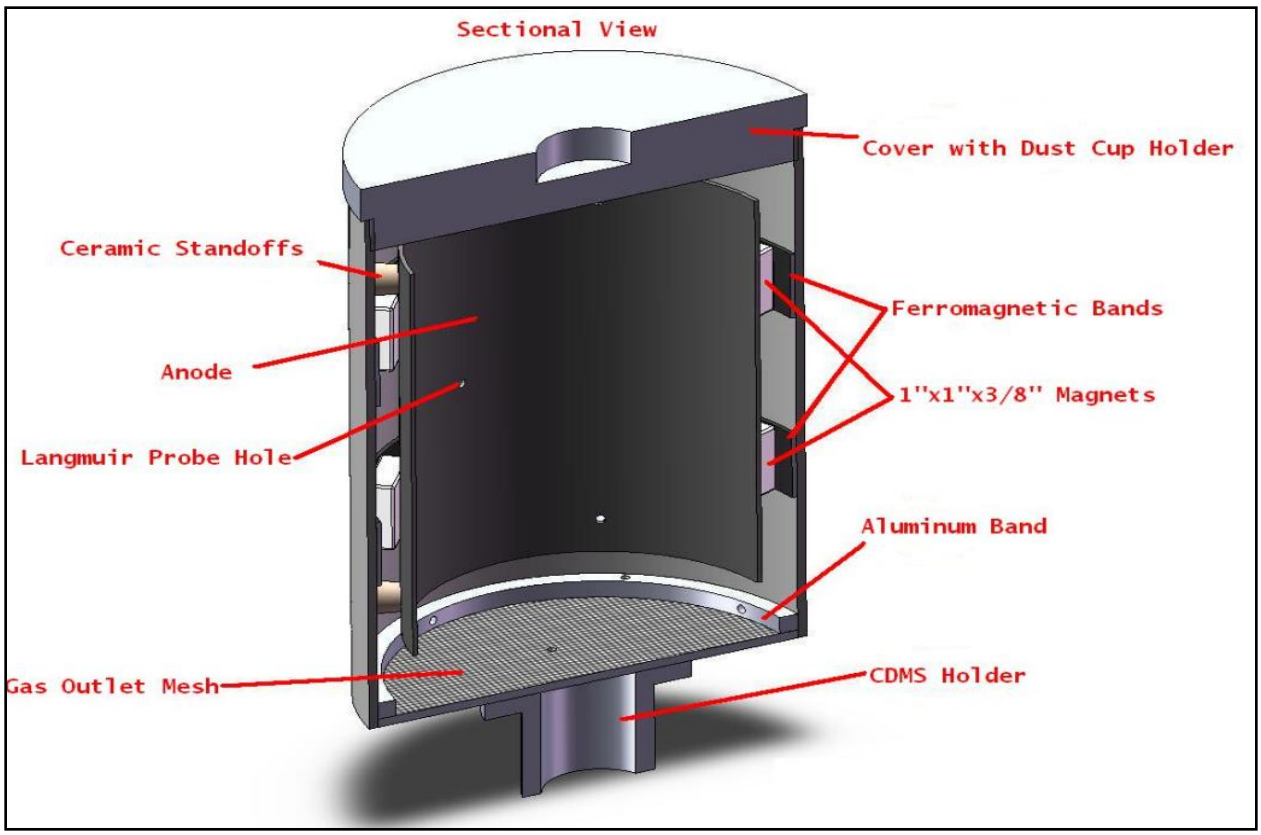

Figure 12: Early Design of Discharge Chamber and Associated Components

The cathode was initially to be mounted directly to the underside of the chambers top cover with a set of 4 ceramic standoffs. To optimize the interaction of the electrons from the cathode and the gas being injected into the chamber, the standoffs were moved to the gas feed ring, which was integrated into the cap (see section 1.2.2).

Castable, machinable ceramic was considered for use as a mounting structure for the electrical isolation of the anode. This system was considered because it could have been formed to match the curvature of the inner wall of the discharge chamber and outer diameter of the anode. Several different methods were considered; including casting ceramic parts directly in the desired shape or obtaining machinable grade ceramic and using CNC controlled machine tools to shape them.

Most of the castable ceramics that were considered imposed unworkable budgetary problems in conjunction with the overall low volume of ceramic that would be obtained. Machinable ceramics were eliminated for similar reasons as well as the possible danger of particle inhalation during the machining process.

The isolation system consists of a set of 8 standard half-inch cylindrical ceramic standoffs. Initial concerns about their ability to conform to the curve of the chamber and anode were addressed by demonstrating that the quarter inch diameter of the standoffs was insignificant when placed against the 5.75 inch and 7.75 inch diameter curves of the anode and inner chamber wall, respectively. These standoffs are shown in Figure 13.

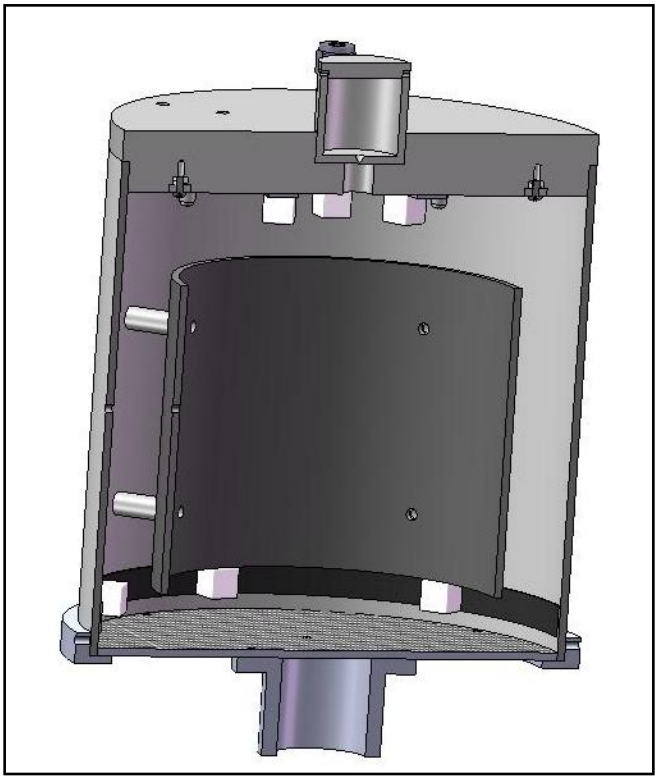

Figure 13: Later Design Iteration Showing Anode Isolation

To ensure a constant electron flow through the chamber, the anode was sized to cover the area from the top of the discharge chamber to the bottom. This allowed the electrons to flow between the cathode and the anode.

To supply electrical power to the chamber, a set of electrically isolated bolts was fed through the top of the chamber. Each bolt was wired directly to the cathode and the anode, respectively. This setup had the advantage of being extremely temperature resistant.

4.2.2 Gas Feed

The first design iteration of gas feed system was a solid tube shaped into a ring and punctured in several places to allow gas flow into the chamber. The gas was to be fed through the top cover of the device and into the tube. The tube was sized to have a larger diameter than the cathode ring, allowing the gas to be injected next to the cathode.

A redesign of the gas feed system resulted in the elimination of the tube. The reason for this redesign was that the first ring design would have taken up too much space inside the chamber. Instead, the system was integrated into the top cover of the device. A Swagelok gas fitting was used for the in inlet into the top of the cover. On the underside of the cover, a groove was machined in to house an aluminum ring sealing over a groove. This ring was designed to have a series of twelve 0.0625 inch diameter holes so that the gas coming into the groove from the Swagelok fitting could be dispersed evenly into the chamber with a total inlet area of $.0184 in^2$. It was intended that the flow through this ring be choked.

The ring also held four standard ceramic standoffs that would protrude down into the chamber. These were used as the mounting system for the cathode. The purpose of this design

was to allow the gas being injected into the chamber to pass directly over the cathode. A detailed view of the ring and cathode mounting system is shown in Figure 14.

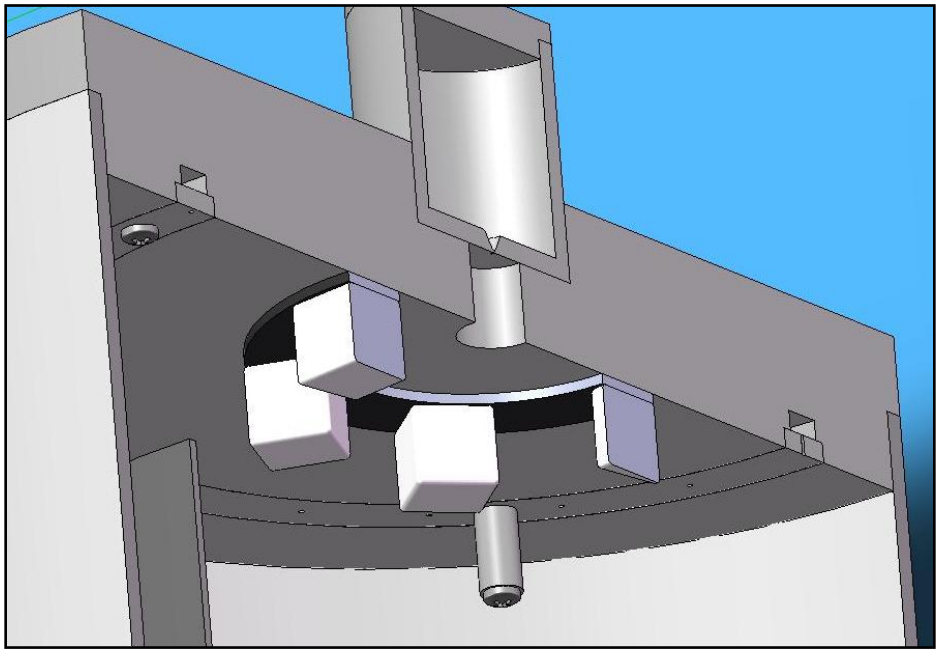

Figure 14: Integrated Gas Feed Ring with Cathode Mounting

4.2.3 Gas Outlet Mesh with Integrated CDMS Mounting

The bottom of the discharge chamber was designed to both let excess gas escape from the chamber as well as allow easy mounting of the CDMS probe. The decision to allow the gas to escape out the bottom was made in order to simplify the design. Though this will allow some of the plasma to escape the chamber, it eliminated the need to design the discharge chamber as a pressure vessel. If there had been no way for the gas to escape it would have built up pressure in the discharge chamber which would have extinguished any discharge. The first design option was to use a piece of perforated aluminum sheet as the "bottom" to the chamber in order to create a surface which the gas could easily pass through. It was decided that this would be round and cut to the inside diameter of the discharge chamber so that when mounted it would be flush

with the bottom surface of the discharge chamber. The SolidWorks model of this piece is shown in Figure 15.

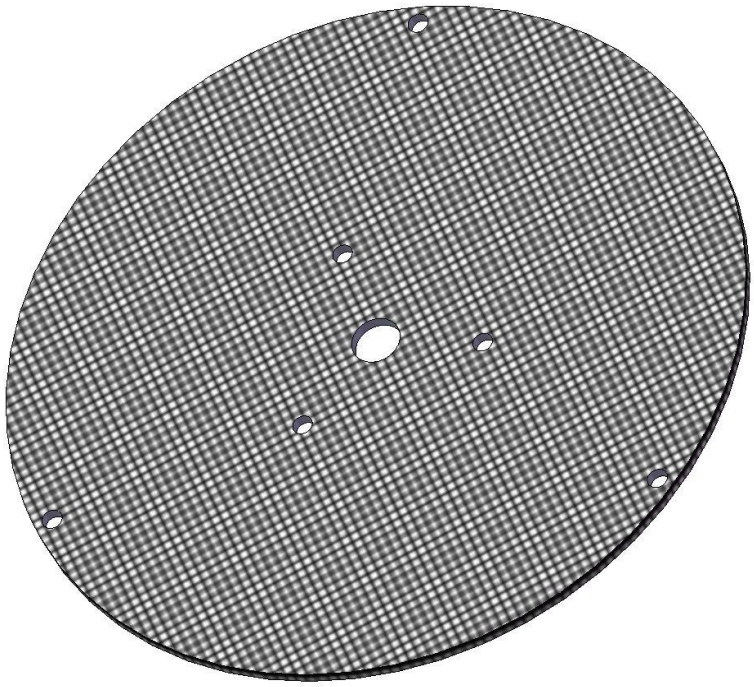

Figure 15: Gas Outlet Mesh

The next design consideration was how this perforated sheet would be attached to the chamber. A circular, L-shaped lip was designed the meet these design requirements. It would be sized such that its inner diameter would be the same as the outer diameter of the chamber, thus allowing it to slip over the chamber creating a flat mounting surface that the perforated aluminum sheet could sit on. The SolidWorks model of this part can be seen in Figure 16.

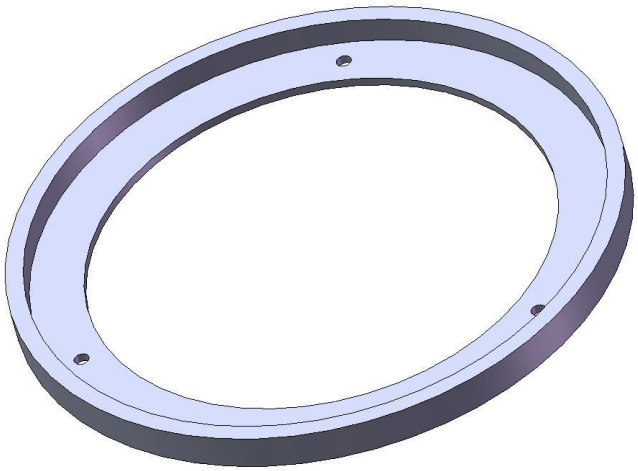

Figure 16: Bottom Mount Ring

The team investigated two different mounting systems in order to attach the L-shaped lip and gas outlet mesh to the rest of the discharge chamber. The first option worked by attaching the screen to the lip using a series of bolts and nuts. Next, six screws and nuts would be used to attach the lip to the chamber from the side. The second option used three structural rods that would run through the entire chamber. At one end they would terminate into threaded holes in the cap, and at the other end they would pass straight through holes in both the screen and the lip. Nuts would then be used to sandwich the entire assembly together. The first option was discarded because of the large number of bolts and nuts required the high likelihood of interference between bolts, and the complications of attaching flat nuts to a curved surface. The second option was far simpler, and optimized the part for machining. An example of the final structural rod design can be seen in Figure 17.

Figure 17: Structural Rod Design

The final component of the gas outlet mesh assembly is the holder for the CDMS. The CDMS must be located below the plasma, and also be aligned with the centerline of the chamber so that the falling dust has a high probability of entering the detector. Because of the relatively small mass of the CDMS, compared to the yield strength of the aluminum screen, it was decided that it could be mounted directly to the gas outlet mesh. The team designed a circular piece with a T-shaped cross section. The center would be bored out to the outer diameter of the CDMS, allowing it to fit inside. Set screws would then be used to hold the CDMS and prevent it from falling out. The SolidWorks model of this part can be seen in Figure 18.

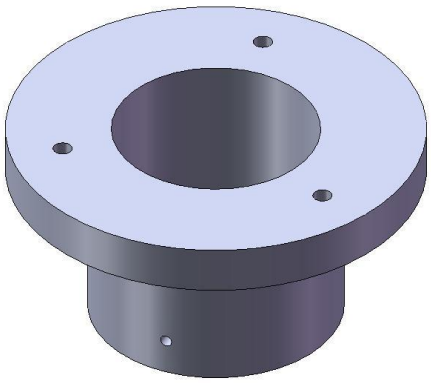

Figure 18: CDMS Holder

4.2.4 Magnetic Field Design

Creating a magnetic field in the discharge chamber with the correct characteristics was essential to this project. As discussed earlier, the neutral gas is ionized due to collisions of free electrons with neutral atoms. The source of these electrons is a cathode at the top of the chamber and travel to an anode in the lower portion of the chamber as illustrated in Figure 19.

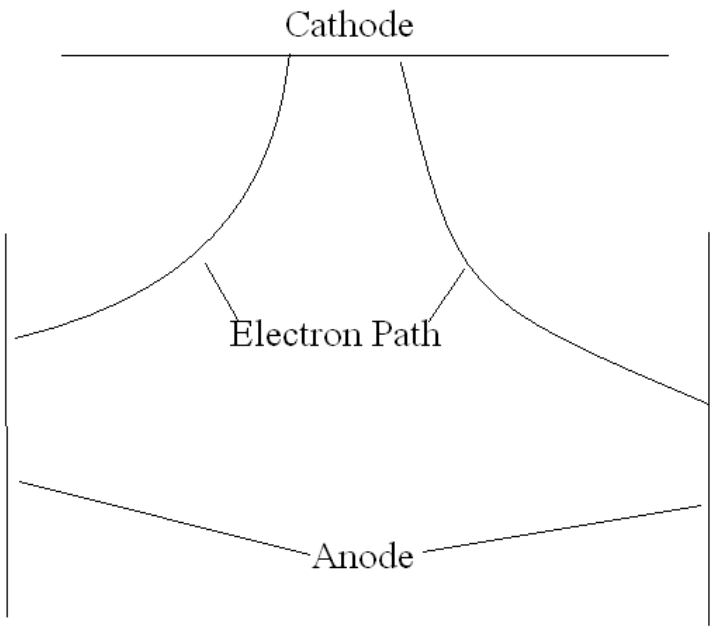

Figure 19: Electron Path

If these electrons follow a relatively straight path as shown in Figure 19 they will have a relatively small number of collisions with neutral atoms and therefore a large fraction of the gas will remain neutral. In order to increase the ionization of the gas, the electron's flight path must be lengthened. By forcing the electron to travel through the gas for a longer period of time, the number of collisions with neutral atoms will increase, thus increasing ionization. One way to accomplish this is to apply a magnetic field to the chamber. According to the Lorentz force equation:

$$F = q(E + [v\ x\ B]) \quad (\text{Eq. } 15)$$

Where F is the force exerted on the electron, E is the electric field strength, v is the electron velocity, and B is the magnetic field strength. If a magnetic field is applied perpendicular to an electric field an electron in this region will follow a helical trajectory. While the electron will

still drift towards, and eventually hit, the anode, the helical path will increase its flight time and its chances of hitting multiple neutral atoms [7].

An important parameter of this helical path is the gyro radius. This describes the radius of the helical trajectory that the electron follows. Should this radius be too large the electron will hit the anode wall before it has the chance to hit many neutral atoms. The gyro radius is given by the equation:

$$R_C = \frac{V_{perp}}{\omega_c} \quad (\text{Eq. } 16)$$

Where v_{perp} is the electrons perpendicular velocity and w_c is the gyro frequency, given by:

$$\omega_c = 1.76X10^{11}B \quad (\text{Eq. } 17)$$

Where B is the magnetic field strength in tesla [2]. For approximation purposes v_{perp} can be said to be equal to the average electron drift velocity, given by:

$$v = \sqrt{\frac{2e\Delta\phi}{m}} \quad (\text{Eq. } 18)$$

Where e is the electron charge, $\Delta\phi$ is the potential difference between the cathode and the anode, and m is the electron mass [8].

In order to determine correct magnet placement for this specific application, a paper presented at the 2007 AIAA Joint Propulsion Conference by a group from Wright State was consulted [1]. The paper provides rules of thumb for magnet location in an ion discharge chamber to get maximum efficiency. Two important conclusions were drawn based on the information in the Wright State paper. First, the number of magnet rings should be limited to

two. By adding more rings to the chamber more cusps are introduced in the magnetic field. Since each cusp is a place where an electron could be lost, more rings means more lost electrons [1]. Also, it was determined that the poles of the two magnet rings should be placed at a right angle to one another rather than parallel to increase electron confinement [1].

Now that the geometry of the magnets placement was decided upon, using the Wright State guidelines, different magnet configurations, such as magnet size and placement, needed to be simulated to see which would be most beneficial. Since the MQP team had no experience modeling magnetic fields they consulted with Mr. Bob Lown, an Engineering Manager at Aster Enterprises in Tyngsboro, MA. Mr. Lown recommended a program called Poisson SuperFish. This program was developed at Los Alamos Laboratories by Ron. F. Holsinger in collaboration with Klaus Halbach. It has the ability to model static magnetic fields in two dimensions [9]. A 2-D drawing of the discharge chamber cross section was created in SolidWorks, and with the help of Mr. Lown it was imported into SuperFish. The original output file developed by Mr. Lown was modified by the team to create several different scenarios. The first sensitivity tested was the effect of changing the radius (r) of the upper magnet ring. Using the guidelines from the Wright State paper, it was known that the ring should have about a one inch radius. Plots were generated for three different scenarios: a single magnet at the center (r=0), a ring with r=0.5 in, and a ring with r=1 in. For this calculation, the diameter of the outer discharge chamber was 6 in, and the magnets were cubes 0.5 in on each side. These values were held constant in order to allow analysis of just the variable being changed. The area between the pink lines represents areas of constant magnetic flux in the chamber. Thus, the number of lines in a specific area represents the flux density, commonly referred to as the magnetic field strength. The more lines there are in a

specific graph area the higher the flux density and therefore the stronger the magnetic field. For all these tests, Samarium Cobalt magnets were assumed due to recommendations by Mr. Lown.

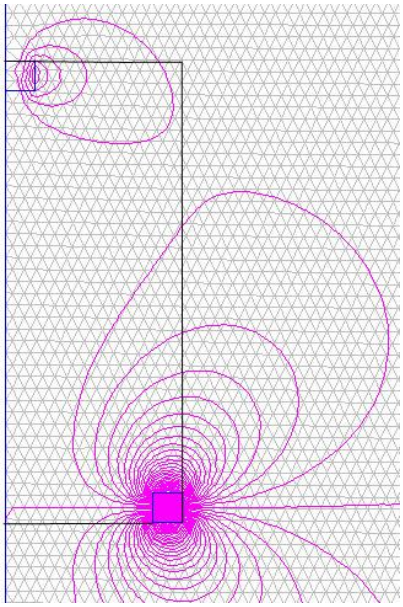

Figure 20: R=0

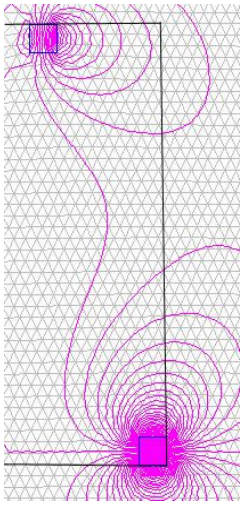

Figure 21: R=0.5

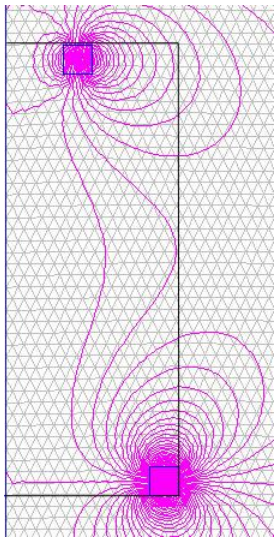

Figure 22: R=1

These plots confirm the findings of the Wright State team. When r=0 the two magnets do not interact significantly and the fields in between them are extremely weak. This field would be ineffective in containing electrons. In the second case, the field is slightly better, with field strength increasing between the two magnets. An even better improvement is seen when the radius is increased to one inch. If the radius was increased beyond r=1 in. the magnetic field would be too weak through the center of the chamber. Of the three, the r=1 in case gives the best field strength distribution. In addition, there are no design drawbacks to making the magnet ring this size. Thus it was decided that the optimal placement of the top magnet ring was at a radius of one inch.

Next, the team had to investigate the effect of discharge chamber size on magnetic field strength. There were two choices available for the outer pipe of the discharge chamber, a six inch outer diameter and an eight inch outer diameter. The eight inch diameter gave a distinct design advantage as there would be more room inside the discharge cavity, but it was unknown how it would affect the magnetic field. For this, magnet size was again set to 0.5 in x 0.5 in and the

radius of the upper magnet ring was set to one inch. These were left constant so only the change in chamber size was investigated. The case of the six inch diameter chamber can be seen in Figure 22 from the previous calculation.

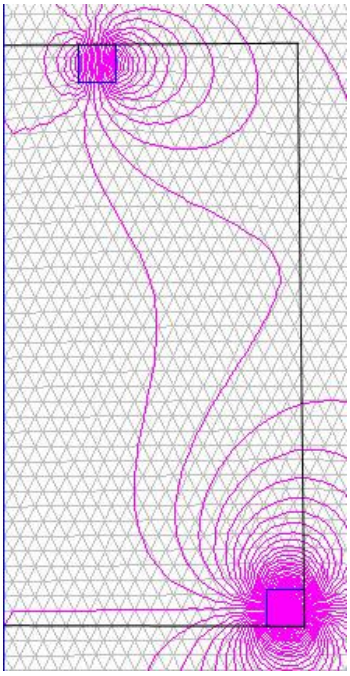

Figure 23: 8 inch Diameter Discharge Chamber

The two configurations show very little difference between the magnetic field strength. To confirm this, the range of the magnetic field strength was determined for each case. For the six inch diameter discharge chamber the field ranged between 0.005 – 0.1 tesla, and for the eight inch diameter discharge chamber the field ranged between 0.004 – 0.1 tesla. These numbers are obtained directly from the program output. This difference is so slight that it would have a negligible difference on electron confinement. Since it gave a significant design benefit at only a slight reduction in field strength it was decided to use the eight inch diameter discharge chamber.

The final test was to determine the effect of magnet size on field strength. When the magnet's size is increased, so is its magnetic strength, and thus the field in the discharge chamber is stronger. This is a trade off, as bigger magnets take up more space in the discharge chamber and cost more. For this test the chamber diameter was set to 8 in, and the upper magnet ring was set to a radius of one inch. Magnet sizes tested were 0.5 in x 0.5 in (seen in Figure 23) and 1 in x 1 in. These were the sizes readily available that would fit in the discharge chamber.

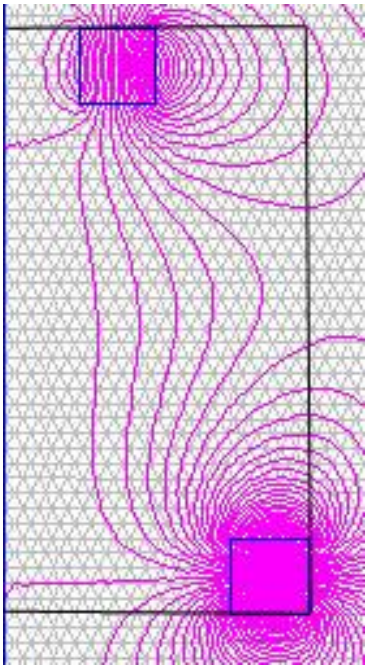

Figure 24: One Inch Magnets

The analysis of this test is slightly more complicated because it requires an analysis of the electron's gyro radius. For the magnetic field to be effective it must contain the electrons within the chamber while causing them to follow a circular flight path. As discussed earlier, the strength of the magnetic field directly influences the radius of the helical path that the electron follows. This gyro radius must be calculated for the two cases to make sure it is not too large. If the gyro radius is too large then the electron will terminate on the anode before it has the opportunity to

collide with a large number of neutral atoms. To calculate the largest gyro radius of the electrons the magnetic field strength is taken from the SuperFish output and used in equation 3. For the inch magnet the largest gyro radius was found to be 0.238 centimeters, and for the half inch square magnet the largest gyro radius was found to be 0.596 centimeters. This was calculated using the equations for gyro radius and velocity stated earlier in this section. The only unknown was potential difference between the anode and cathode which was set as 50 V. Both of these numbers indicate electron paths well within the limits of the 8 inch diameter discharge chamber. Therefore, due to their design benefit and much lower cost, the half-inch square magnets were selected.

After running all three simulations it was determined that the upper ring should be placed at a radius of one inch, that an eight inch diameter discharge chamber should be used, and that half inch cube magnets would provide the necessary electron confinement. Mr. Paul Lituri of BJA Magnetics was contacted, and using these guidelines a quote was drawn up for the correct size and type of magnet needed.

4.2.5 Mounting System

The mounting system for the discharge chamber was designed around the vacuum chamber in WPI's Higgins Laboratory room 016; the chamber is 50 in diameter and 72 in long. To support the discharge chamber in the middle of the vacuum chamber, two H-frame structures were assembled using aluminum fractional T-slotted rails. The H-frames were connected to parallel rails in the bottom of the chamber.

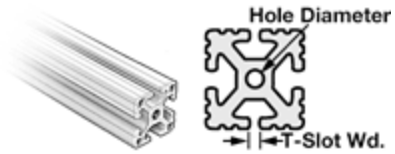

Figure 25 - Aluminum fractional T-slotted framing system

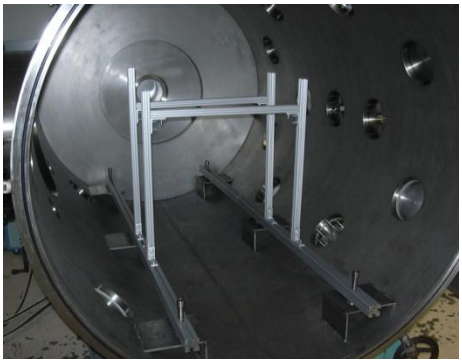

Figure 26: Supporting structure inside the vacuum chamber

The rails are connected together by bolts going through L brackets and screws going through tapped holes at the end of the rails.

Figure 27: L Bracket

Two blocks attach to the horizontal rails and then the discharge chamber. The blocks are curved on one side to match the curvature of the discharge chamber and are attached to the rail and discharge chamber by screws through tapped holes.

A strip of sheet metal spans the distance between the horizontal rails. The sheet metal supports a stepper motor which hangs underneath. The stepper motor is there to move the Langmuir probe inside and out of the discharge chamber. This design is covered in depth in the Langmuir probe assembly section. The assembly that will be inside the vacuum chamber can be seen in Figure 28.

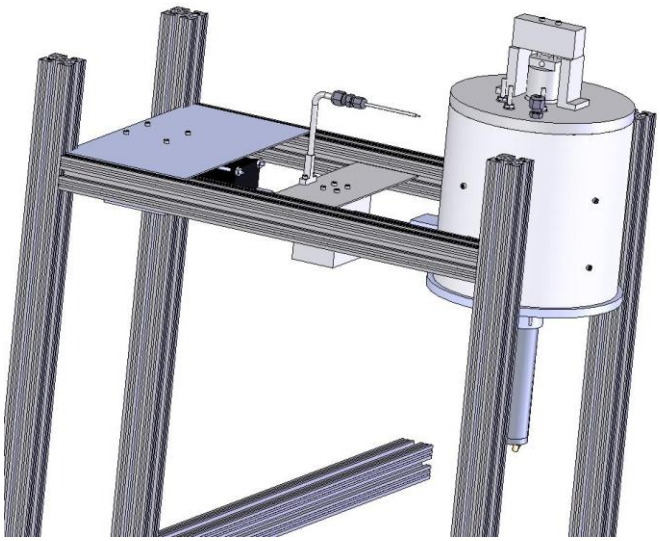

Figure 28: Entire structure including mounting frame, discharge chamber and probe positioner.

4.3 Particulate Injector

The purpose of the particulate injector is to hold the dust particles and then release the dust into the discharge chamber. The particulate injector began as a 1.5 in diameter aluminum cup with a small hole in the middle to allow the 70 micron size spheres of alumina powder dust

to fall through. A vibrating motor was required to shake the particulate injector so that the dust would fall through the hole. It was decided to use the same type of vibrating motor found in cell phones because it is small and inexpensive. The motor has a small spinning offset weight. A re-design was needed after further thought of how the particulate injector would hold the vibrating motor and release the dust. To attach the motor to the particulate injector, a boss was added with a hole for the motor to slide into and secured with a set screw. The size hole needed for the dust was not known so the particulate injector was designed to have a removable bottom cap which had the hole in it to allow caps with different sized holes to be interchanged. On each removable cap there is a conical shaped depression to act as a funnel for the dust.

The planned procedure calls for the dust to be loaded into the opening; the cap placed over the opening and turned over so the hole faces downward to allow dust to fall out.

The particulate injector needed to be lifted up so it did not rest on the discharge chamber's cap; this was done to keep it from transferring too much vibration into the discharge chamber. Two aluminum blocks with a strip of aluminum between them lift the particulate injector off the cap. Two tapped holes in the particulate injector allow it to be attached underneath the aluminum bar in-between the two blocks with screws.

The bar of aluminum that stretches between the two blocks has a thickness of 1 in. It has two clearance holes for the screw to pass through and screw into the particulate injector. The clearance holes will allow the particulate injector vertical motion caused by the vibrating motor in the particulate injector and at the same time restrict any horizontal motion. This is important so the dust coming out of the particulate injector goes through the hole in the cap and into the discharge chamber. The entire assembly can be seen in Figure 29.

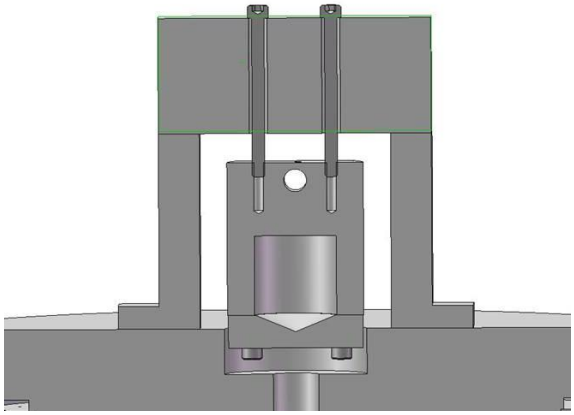

Figure 29: Particulate injector and structure.

4.4 Langmuir Probe Assembly

As discussed earlier in this report, a Langmuir probe will be used in order to determine the characteristics of the plasma created in the discharge chamber. Due to the fact that the plasma properties will most likely vary through the chamber, it was desirable to create a system so that the Langmuir probe could be moved in and out of the discharge chamber. This will allow the probe to make readings at different points within the chamber and collect data on how the plasma properties vary. The team had previously decided that the probe would have to be mounted on a platform outside of the discharge chamber due to the fact that the probe risks becoming damaged due to long exposure to the plasma environment. The challenge was to design a way to move this platform so that the position of the probe could be precisely controlled. A previous MQP team had worked on a similar problem to create a probe positioning system to investigate pulsed plasma thrusters. This team decided to use stepper motors to drive a positioner and bought a controller card that interfaced with LabView for control. Since this controller was already set up and mounted on the instrument rack near the chamber in HL016, it was decided to also use stepper motors that could interface with this board. The stepper motor would be attached to a

block and platform assembly that would be attached between the two cross bars of the mounting frame.

A precision lead screw will be used to create the linear motion. At one end the screw is attached to the stepper motor, which will drive it. At the other end it terminates in a bearing, attached to the discharge chamber, which allows it to freely rotate. An aluminum block will have a hole drilled through it, tapped at the same thread pitch as the lead screw. This block will then be threaded onto the lead screw. A small platform that will stretch between the uprights of the chamber mounting frame can then be attached to this block. This entire assembly will then slide back and forth along the rails. The threaded aluminum block will act as the interface between the moving platform and the lead screw, and the platform will act to balance everything so that the motion remains linear. The Langmuir probe can then be mounted on this moving platform.

4.5 Fabrication Process

Due to budget restrictions and the desire to have this project provide a practical engineering experience, all parts designed for the discharge chamber were manufactured by the team. This initially posed a problem as none of the team members had any experience with either the manual or Computer Numerically Controlled (CNC) machines available for student use at WPI. The team found a large network of support through Neil Whitehouse, head of the Higgins Labs shops. In the first week of B-term, Neil arranged for a short demonstration in the shops, going over basic operation of the manual machines. Neil also offered a weekly course to help students learn how to progress from design to actual machining. Both of these courses were invaluable to the team. Neil and his work study students were available to answer any questions while the team was working in the shop and to helped provide solutions to manufacturing

problems. It was realized early on that the manual machines would not be sufficient to complete all of the parts the team designed, so while Joe, Brian, and Bill concentrated on learning the manual machines, Conn spent time learning how to develop parts for CNC machining using GibbsCam.

Four machines were used for the majority of machining tasks. The first was a DoAll Model 200V Vertical Milling Machine. This manually operated mill works on three axes and is driven by a 2 HP motor. The second was a DoAll Model LD1360 Engine Lathe. This is a manually operated lathe that is rated at 5.12 HP. The team also made use of the horizontal band saw. This machine helped the team cut raw stock to length quickly, when surface finish either did not matter, or could be quickly improved on the mill or lathe. When CNC machining was necessary the HAAS TM-1 Tool Room Mill in the Higgins shops was used. This three axes computer-controlled mill is driven by a 7.5 HP motor.

Fabrication of parts for the discharge chamber was based on previously created SolidWorks models. Though these models were well made, the dimensions were not always exactly followed. Variations came from a number of places. Most often, the team's inexperience with the machines resulted in small variations from the desired dimension. If a dimension was non-critical and the part would still function correctly, the new dimension was used even though it differed from the SolidWorks model. These changes were then used to update the SolidWorks model to reflect the most current design. Variations also occurred when the tools were not available to accomplish the desired feature. Since the team had little to no knowledge of machining when the SolidWorks models were created, some parts were not possible to easily machine with available mills and drill bits. In such a case the part was re-examined to see how a standard sized hole would affect the parts functionality. A final source of variation came from

the fact that a perfect fit in SolidWorks did not necessarily correspond to two parts fitting in the real world. For example, the CDMS mount was designed to have an inner diameter of 1.5 in, the same as the outer diameter of the CDMS. While this worked in SolidWorks, in real life the fit was too tight to be used in functionality. Therefore the inner diameter of the CDMS mount was modified so that the CDMS would fit into it easily.

Another important part of the machining process was material selection. As a general rule, aluminum was used for the parts that needed to be machined, unless there was a pressing reason not to. Aluminum was chosen because it is lightweight and easy to machine. Since it is a relatively soft metal it can be machined faster and is more forgiving of mistakes (i.e. tools bits are less likely to break due to errors in cut depth and speed). A bonus to this was that aluminum is relatively inexpensive and was readily available in many different forms in the WPI stock rooms.

Other materials were used occasionally throughout the project. First, steel was used to make the magnetic rings, since the magnets would stick to it, eliminating the need for vacuum compatible adhesives. The other non-aluminum material used was the plastic, Delrin (Dupont's trade name for acetal resin, a hard, temperature resistant polymer). This was used for parts that needed to be electrically isolating in the CDMS. If certain parts became electrically connected it could cause the probe to give false readings.

In this section the specifics of how each part was manufactured will be explained. This should serves as a practical guide for anyone to recreate the parts made for this project.

4.5.1 Framing System

The frame for the discharge chamber – though needing careful thought – was one of the easiest fabrication projects for this MQP. After designing it, special bars had to be ordered from MSC Industrial Supply. These bars are made to mount with ease. These bars are two parallel H-frames, and each was 1 inch by 1 inch by 8 feet long when shipped to WPI. They are easy to use because special bolts can be inserted and the end of the bars can be tapped. A bolt can then be screwed into the end of the bar to to get a specific angle.

After the team received the two 8 foot long bars, we cut them to the desired lengths using horizontal band saw. There are holes in the ends of the bars, and the team then tapped them as needed, and started to put the bars together in the H-frame configuration.

After the initial construction, it was noted that the frame would wobble. After examination, it was determined that the bolts provided with the aluminum rails were too small to fasten the frame system together securely. Larger carriage bolts were then used to securely assemble the frame.

4.5.2 Discharge Chamber Shell

The original stock for the main chamber was an 8 in diameter tube of length 12 in and wall thickness of 0.125 in. To cut the tube down to 8 in a mobile horizontal band saw was used. Unfortunately, this saw was not big enough to cut through the 8 in diameter in one pass and resulted in an uneven cut. The manual lathe was used to try and clean up the tube by using a cut-off tool; however it was also unsuccessful due to the tube's size. Peterson Steel (Worcester, MA) was contacted to try and cut the tube for the team, however they said the diameter was too big

and the wall thickness too small to safely cut the stock. As a result of all this, the stock was scrapped and an order was placed for 8 in diameter tube, custom cut to a length of 8 in.

The 8 in tube required eight holes to be drilled in the wall to attach ceramic standoffs which would hold the anode. Four holes were evenly spaced at 90 degrees to each other at one length from the end of the tube. Four more holes, also evenly spaced at 90 degrees to each other, were at a length offset from the previous four holes. To cut these holes the tube was placed in a horizontal rotary chuck on a manual milling machine. It was necessary to drill perpendicular to the surface of the tube, so while the tube lay horizontal in the chuck, a marble was placed inside the tube. The marble rolled to the bottom most part of the tube, and this point was marked. The tube was rotated 180 degrees and the drill was lined up with the marked point. A block of wood was placed under the tube, at the far end, to keep it from flexing when being drilled. After drilling the first hole, the tube was rotated 90 degrees, and another hole was drilled. This was repeated until there were four evenly spaced holes in the tube. The table connected to the milling machine was then moved four in to drill the next 4 holes.

4.5.3 Discharge Chamber Cap

The fabrication of the cap required multiple, complex steps on the CNC milling machines. Initially, an individual on the team found aluminum stock that was 12 in in diameter, and approximately 2 in thick. However, the stock was too large to be machined safely and would have resulted in a substantial waste of material. Two lessons were learned: First, it was important to have the proper aluminum stock size, which was 8 in in diameter by 1 inch thick, and second, the CNC milling machine was needed to properly machine the part.

One more choice had to be made for the fabrication of the part. Should it be CNC milled or CNC lathed? The CNC mill was going to be used because there were certain cuts that

couldn't be done on the lathe. This allowed the team to simplify the manufacturing process into three main parts – one program was for the top of the cap, the other for the slotting and drilling, and the last for the lip on the outside to fit on top of the discharge chamber.

At the beginning of the project, no individual in the group knew how to operate the CNC mill or lathe. This proved to be the first major hurdle to machining the cap. It was quickly discovered that the CNC machines, though automated, required certain skills, such as knowledge of a program called GibbsCam. This program is designed to take CAD files and let the user set different tool paths. GibbsCam then writes the machine code needed to operate a CNC machine.

A few major lessons were learned: first, stock is never, ever level. This can be solved by facing with a .02 inch depth with the CNC machine. Second, the team also learned that GibbsCam was unable to set the spindle speed with the calculators in the program. All the speeds needed to be calculated using a program provided by Mr. Neil Whitehouse.

The code for slots and drill holes then had to be created for the underside of the cap. This proved to be a challenge because the team did not know of a process called 'contour' existed in GibbsCam. After some outside help, the team was able to understand how to set the needed tool paths for both the slotting as well as the profiling that needed to be done.

Another issue encountered was the clearance on the parts. The way the part was bolted to the table, it risked breaking a bit. However, a conservative estimate of .5 in for rapid movement was chosen. However, in retrospect, 1 inch clearance should have been used to fit into the margin of error.

Overall, the piece came out well. The cap fits all required tolerances and serves all of the different functions it needs to fulfill.

4.5.4 Bottom Magnet Ring

To create the bottom magnet rings, a 12 in x 12 in, 0.0625 in thick steel sheet was used. Two 0.5 in wide strips were sheared off of the stock and then manually curved and forced inside the main chamber tube. Once curved, and held inside the main chamber tube, 2 points near the end of the steel strip were marked. Two 6-32 clearance holes were then drilled in each of the metal strips so they could be bolted to the inner wall of the discharge chamber. This operation was repeated for each metal strip. The metal strips were held back in place on the outside of the tube and points on the tube were marked by the holes in the metal strips. The holes on the outer tube were then drilled using a hand drill. The strips were then placed inside the main tube, and fastened in place with 6-32 nuts and bolts.

4.5.5 Bottom Ring

The bottom ring of the chamber provides support for the mesh as well as a means to hold the discharge chamber components together. This bottom ring is 8 in ID, just enough to fit snug on the outside of the discharge chamber. The OD is 8.5 in, allowing a lip of 0.25 in around the entire chamber. The 8 inch circle and the three holes with a diameter of 0.209 in had to be precision milled. The holes were required to mount the bottom ring to the

Though simple in design, the ring was a challenge to create for a number of reasons. A circular recess needed to be machined out of a piece of aluminum stock to a diameter of 8 in. The team decided to make this part on the Computer Numerically Controlled (CNC) Vertical Mini Mill machine. It was considered making this part in a manual vertical mill, but there were mounting issues with taking square 12 inch stock and milling a perfect circle out of it. The roto chuck could not be used to create the circle, because there was no way of clamping down the

square stock in the circular chuck, and it is nearly impossible to accurately mill a circle freehand if one clamps the square stock to the table.

Unfortunately, it was impossible to do this using the CNC Vertical Mini Mill. No matter where the stock was placed, the machine did not have enough travel to probe it. A more effective way of probing the part was needed.

It is possible to probe the part by placing the probe over the estimated center of the stock. Neil Whitehouse, the manager of the shop, showed the team how to manually set the origin.

When machining aluminum with an end mill, it is best to use a 2-3 flute bit with a diameter of approximately 0.5 in. A new bit in the Washburn Labs, which was 0.5 in, had 5 flutes. This can have certain advantages. Mainly, the feed rate in inches/minute can be increased since more flutes result in more material removed per one rotation. This bit was used, but with adverse consequences. Since there were so many flutes, the chips couldn't clear fast enough. This created an unprofessional finish and sloppy tolerances. However, the function of the piece was maintained despite the mistake in using this particular bit.

Though the team now had a circle in the part with the three 0.209 inch diameter holes, the outer diameter of the part was still 12 in by 12 in. The easiest way of achieving the 8.5 inch OD circle was to put the part in the vertical manual mill with the indexing chuck and was machined down to the 8.5 in OD. Overall, the part came out well. The finish was less than optimal because of the 5 flute 0.5 inch end mill that was used, but the effectiveness of the part was not affected.

4.5.6 Gas Outlet Mesh with Integrated CDMS Mount

The bottom section of the discharge chamber consists of three parts: the bottom mounting ring, the gas outlet mesh, and the CDMS mount. Due to the fact that the bottom ring had some

precise features, it was decided to manufacture it using the CNC machines which was covered in the previous section. On the other hand, the gas outlet mesh and CDMS holder were simple parts to manufacture and were created using manually operated machines.

The raw stock for the gas outlet mesh was a 12 in x 12 in piece of 0.125 in thick aluminum mesh, purchased from Online Metals (Seattle, WA). The outer tube of the discharge chamber was placed on this sheet and a permanent marker was used to mark a circle corresponding to the inner diameter of the tube. Since this was one of the first machining operations the team worked on it was decided to use the jigsaw to cut out the circle because it required relatively little training to use. The jigsaw proved to be more difficult than originally thought, and multiple blades were broken before an approximate circle was cut out of the raw stock. It was decided that using the mill combined with an indexing chuck would be the best way to circularize the part. First, a hole was drilled through the center of the existing part. This hole would serve a double purpose, ensuring the dust would have an unrestricted path into the CDMS, and also allow the part to be easily mounted for machining. Next, a sacrificial piece of wood having roughly the same diameter of the screen was found, and the screen was bolted to it through the previously drilled hole. This wooden mount would lift the screen above the rotary-chuck and allow a mill to be run around the edge of the part. A half-inch end mill was then brought to the edge of the piece and rotated around to circularize the piece. After each pass the piece was inspected visually and test fitted into the chamber until the team was satisfied that the piece was roughly circular and would fit into the chamber appropriately.

The CDMS holder was manufactured using the horizontal band saw, the manual lathe, and the manual mill. The raw stock for the piece was thick walled aluminum pipe with a 2 in OD and 0.5 in ID, obtained from the Higgins Labs stock room. A piece of stock much longer than

needed for the piece was chucked up in the manual lathe. First, a boring bar was used to widen the inner diameter of the pipe until it was slightly bigger than the 1.5 in OD of the CDMS. This was to allow the CDMS to slide easily in and out of the mount while preventing excessive wobbling. Next, a turning tool was used to cut down the outer diameter on all but 0.25 in of the desired length of the part to create the lip that would be used to mount the piece to the gas outlet mesh. The piece was then removed from the lathe and placed in the horizontal band saw. The blade was positioned to cut the stock to slightly longer than the actual piece would be to allow for facing operations. The piece, now cut to size, was placed back in the lathe and the side cut by the band saw was faced in order to obtain a flat, good finish. This piece was then placed in the indexing chuck on the manual mill. Three through holes for 6-32 screws were drilled in the mounting lip at 120° intervals, all at the same radius.

4.5.7 Cap Interface – Electrical and Gas Feed

The cover of the discharge chamber serves as the interface for many of the apparatus' vital functions. Among them are the electrical feeds and the argon gas feed. The manufacturing of these feed throughs were done simultaneously, as many of the components involved have important functions for both the electrical and the gas feed.

First, four holes were drilled through the top of the cap. Three evenly spaced, 0.25 in holes were drilled for the electrical feed through at a set radius from the center of the cap. This was accomplished by mounting the part on an indexing (rotary) chuck on a manual mill. The electrical feeds were then assembled by inserting 2 in long 10-32 threaded rods though 1 in ceramic bushings and inserting them into the newly drilled holes. They were then locked into place by sandwiching ceramic washers between the ceramic bushing and nuts on the top and

bottom of the cap. The result is a set of electrically isolated terminals on the inside of the cap that can provide current and electrical bias to the cathode and anode, respectively, inside the discharge chamber.

The fourth hole was drilled and tapped using an indexing chuck on a manual milling machine. The hole was drilled and threaded to accept a 1/4 - 20 Swagelok fitting for the gas feed interface. This hole was precisely located to open into the gas feed ring on the underside of the cap as shown in Figure 30.

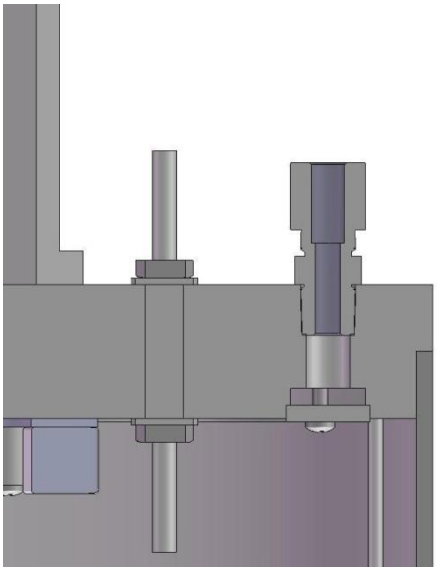

Figure 30: Gas Feed Interface

One of the most vital components of the cap interface is the aluminum gas feed system cover used as a mounting point for the cathode and to evenly disperse argon into the discharge chamber. A prefabricated aluminum ring was used for the cover of the gas feed system. To machine the cover out of this ring, eight clearance holes were drilled at 45 degree intervals along a constant radius of the ring. Using 4 of the 8 clearance holes, the cap was bolted into the pre-made groove on the underside of the cap. The bolts were screwed into four tapped holes located within the cap. The other four holes were made to accept screws to attach a set of 4.5 in ceramic

standoffs onto which the cathode filament was mounted. A set of twelve 0.0625 in holes was then dilled with an even spacing and a set radius on the ring. These holes serve as the inlet for gas dispersion. The cathode and anode were then wired to the appropriate electrical feeds on the underside of the cap. The result of the fabrication process is a gas discharge ring that doubles as a mounting point for the cathode. All electrical and gas feeds are integrated directly into the cap interface.

4.5.8 Anode

The anode located inside the discharge chamber is a curved sheet of aluminum that has been electrically isolated from the chamber and can be electrically biased for plasma generation. The anode is isolated from the wall of the chamber by a set of eight 0.5 in ceramic standoffs fixed to the inner wall of the chamber. Sets of two standoffs are spaced every 90 degrees along the inner wall of the chamber.

To construct this component, a sheet of .0625 in sheet aluminum was measured, marked, and sheared into a rectangle whose width was to be the total height of the anode (6 in) and whose length corresponded to the expected circumference of the anode once it was rolled into its final, cylindrical shape. The circumference of the anode was calculated by subtracting the thickness of the 0.5 in ceramic standoffs that isolate it from the inner wall of the discharge chamber from the inner diameter of the discharge chamber. A basic geometric calculation then yielded the needed circumference.

The location of clearance holes that are used to bolt the anode to the standoffs were calculated and marked onto the sheet metal using a simple scale and marker. The holes were then carefully drilled with a drill bit using a manual milling machine. In order to mount the sheet

metal in the mill, a piece of sacrificial scrap wood was secured in the machine and the sheet metal was then adhered to its surface. At the edges, where the ends of the anode would join together once shaped into a cylinder, a set of four notches were cut instead of holes. These notches were designed to overlap and create the clearance holes for two of the standoffs. This design feature allowed for considerable relaxation of tolerances for the positions of the holes. The anode was shaped into a cylinder by rolling it along the outside of the discharge chamber. It was then fit into place and bolted to the eight ceramic standoffs. The electrical bias is provided by wiring the anode to one of the electrical interfaces that runs through the cover of the discharge chamber.

4.5.9 Particulate Injector

The cup that holds the dust started as a 12 in long 1.5 in diameter aluminum rod. The outer edge was faced on the manual lathe to improve the finish. A 0.5 inch hole was drilled through the open end of the rod while on the lathe to a depth of 1.5 in. Using the horizontal band saw, a 2 inch piece of the 12 in rod was sliced off.

The piece was put on a manual milling machine with a rotary chuck to create the boss on top of the cup. A 0.5 in end mill was used; making passes of a depth 0.1 in, for a total depth of slightly over 0.25 in Passes were made on 2 sides of the piece, leaving a rectangular shaped boss. The cup was then placed on its side, so that a 0.25 in hole could be drilled perpendicular to the boss; this would be used to mount the vibrating motor. A small hole on the top of the boss was drilled and tapped so that it could receive a set screw to hold the vibrating motor in place. Two larger holes were drilled and tapped at an equal spacing on either side of the set screw hole so that the cup could be mounted to a cross beam. Three holes were drilled and tapped along the

bottom of the cup, the open end, for the cap to attach to. These holes all have the same radius from the center, and are separated by 120 degree angles.

The cap to the cup was made from the original 12 in long 1.5 in diameter aluminum rod. The rod was placed on the manual lathe and a boring bar was placed at an angle so that when plunged, it created a cone section in the rod. The piece was then cut off with a thickness of 0.25 in. A total of three caps were created using this method, so that different outlet hole sizes could be tested.

The caps were placed in the manual milling machine to create three clearance holes, for a 6-32 screw, on the outer edge. The radius from the center is the same radius as used on the bottom of the cup and are also set 120 degrees apart, using the rotary chuck, to line up perfectly. The cap was then screwed into the dust cup with three 6-32 screws.

To create the structure which supports the cup and cap assembly, three blocks of aluminum stock were used that were found in Higgins scrap room. The finished assembly consists of a single cross beam atop two L-shaped brackets. The cup which holds the dust is mounted underneath the cross-beam. The top crossbeam block had two clearance holes drilled for long screws to slide into. These holes had to be very exact so the screws that would go in the holes would have minimal lateral movement, to limit side-to-side motion of the shaking cup. Two clearance holes for a 6-32 screw were drilled on either end of the crossbeam to attach to the L brackets.

The uprights were created by machining the two other aluminum blocks into L shaped supports. To accomplish this, the blocks were set in the vice, on top of parallels to lift it up evenly, so that the side with greatest area was facing up. The end mill was set to the desired depth and the passes were made back and forth, using the side of the end mill as the cutting edge.

A hole was drilled and tapped on top of the uprights that would match the clearance hole on the crossbeam so that the crossbeam could be screwed into the L-brackets. A clearance hole for a 6-32 screw was drilled through the base of each upright that would allow the entire structure to be attached to the cap of the discharge chamber.

4.5.10 CDMS

All parts for the CDMS were created using a combination of CNC and manual machining. The raw stock for all metal pieces was a piece of 2 in OD aluminum rod found in the Washburn Shops stock room. This piece was chucked in the manual lathe and a turning tool was used to reduce the OD to 1.5 in. The stock for the Delrin parts of the CDMS was a 2 inOD rod of Delrin taken from the Higgins Labs stock room. Similarly to the aluminum stock, the Delrin rod was chucked in the manual lathe and turned down until its OD was approximately 1.38 in to allow it a sliding fit inside the CDMS cover tube. After the stock was turned to size a series of GibbsCam files were written to create the G code for the parts. These files included operations for all the required holes that needed to be drilled in the CDMS parts. This code is a series of instructions that the CNC machine can read and translate into machining operations. This was done to make sure that the precise tolerances needed for the CDMS could be maintained, something that would be difficult on the manual machines.

The general procedure for creating a CDMS part began by placing the raw stock in the CNC machine. The appropriate program would then be run to drill the correct holes for the piece being made. The stock would then be chucked up in the manual lathe. A cutoff tool would be used to cut the raw stock at the appropriate length to create the individual disc parts of the

CDMS. The remaining stock was put back into the CNC machine, with different code, to make the next part.

The back piece of the CDMS had a slightly more complicated procedure. This piece was first placed in the CNC machine, and the holes were drilled into it, making the top of the stock the back of the piece. This posed a problem, as the front half of the piece needed to be cut down to an outer diameter of 1.39 in to allow it to fit into the CDMS cover. Since the part was very small it was not possible to simply cut the piece off and put it back in the lathe facing the other direction. To machine this feature, the stock was chucked up in the manual lathe, and a diamond tip cutter was moved to approximately half an inch back on the stock. It then cut into the stock 0.11 in and was moved toward the chuck. This created a rough pocket in which a normal turning tool turned backwards could be used. The backward turning tool was used to cut away from the chuck and bring the front half of the piece down to the required outer diameter. As with the other pieces, a cutoff tool was then used to remove the piece from the stock.

4.5.11 Langmuir Probe Assembly

The Langmuir probe serves as the primary means of evaluating the level of ionization of the gas inside the discharge chamber. To use it, an assembly was constructed that would allow up to 8 in of linear travel from the outer edge of the discharge chamber, into the plasma field, and back out. The assembly that was designed for this purpose is a stepper motor attached to a lead screw and bushing that can be controlled remotely and is integrated into the framing system that supports the discharge chamber when in vacuum.

A stationary mount for the electric motor was created by bolting an aluminum block to the underside of a set of three aluminum plates. The plates were sheared from a sheet of 0.0625

in aluminum stock with a metal shear. The plates were then bolted to the tops of the H-frames, the same rails that support the discharge chamber. The motor was then bolted to the vertical face of the block that was oriented towards the discharge chamber when in vacuum as shown in Figure 28. Another set of sandwiched plates supported the Langmuir probe itself. This set of plates was slid into the framing system to allow linear travel only along the radial axis of the discharge chamber. An aluminum block was mounted beneath the plates and houses a threaded bushing. This bushing represents the interface where force is transferred from the stepper motor to move the probe.

The two aluminum blocks (one to support to stepper motor, one to support the Langmuir probe itself) were constructed out of stock aluminum using a manual mill with a 0.375 in diameter flat end mill. The stock was faced down to the appropriate sizes for each respective component (see design section on Langmuir Probe Assembly). Because of the orientation of the cutting tool, and the irregularity of the stock that was used, special care had to be taken to ensure that all the faces on the blocks were perpendicular to one another. Failure to take such precautions would have resulted in the finished blocks being irregular parallelepipeds. To mount the motor in place, an edge finder was used to find the center of the mounting block, and then calculations of the motors' dimensions were done to find the precise location of each hole relative to the center of the block.

A 1/4-20 lead screw was then mounted on the output shaft of the electric motor using a universal joint interface, through the threaded bushing, and connected to a stationary bearing using a double sided 1/4-20 female adapter. The bearing was press fit into an aluminum block that was contoured with a CNC vertical mini-mill to fit along the outside wall of the discharge chamber. A pocket was then machined out of it to receive the bearing.

The probe itself is a high purity tungsten conductor, fed through an alumina insulator, which is supported by a 0.25 in stainless steel tube. Inside the alumina bore hole, the tungsten filament is press fit so that it makes contact with some fine gauge magnet wire which is fed through the entire length of the alumina and the stainless steel support. The alumina insulator protects the delicate filament while in the plasma and prevents current from being collected anywhere other than the exposed end. The support tube was bent 90 degrees with a standard tube bender. It was then mounted to the top of the set of sliding plates with a specially designed mounting bracket. The bracket is a T shaped piece of aluminum with two clearance holes so that it can be bolted to the top of the sliding plates. To machine it, a piece of stock was mounted into the manual mill. A 0.375 in face mill was then used to shape the stock into the desired T shape. The bracket was then mounted vertically and the mounting holes were drilled into its base. A pocket was then drilled out of the bracket to receive the tubing that houses the Langmuir probe filament.

5. Conclusions

Unfortunately, due to mechanical problems with the one of the mechanical pumps used to evacuate the vacuum chamber, testing of the discharge chamber was not possible during the standard three-term duration of the MQP. Despite this, some important conclusions can be drawn about the design and manufacture of the chamber.

First, parts need to be extremely carefully planned during the initial design phase of the project. One issue the team had was designing parts that were extremely difficult, if not impossible, to machine. These complications arose from the use of non-standard hole sizes and dimensions with unnecessarily precise tolerances. With respect to the former, no available drills could be used, forcing parts to be redesigned in the machine shop. The tight tolerances in the initial designs considerably increased the machining time required for parts, in most cases, these tight tolerances may not have been necessary. Sometimes, the capabilities of the machines were overestimated, resulting in loss of machining time and rendering the stock unusable. Had these factors been accounted for early on in the design process time, stock, and money could have been saved.

These problems in manufacturing were caused by the team having little to no training in the machine shop prior to this project. This resulted in an extremely steep learning curve that had to be overcome before useful parts could be manufactured in a reasonable timeframe. Had the team received prior instruction, before the project began, the manufacturing phase could have been shortened considerably. Any future team undertaking a similar project would benefit from acquainting themselves with the machine shop before beginning their manufacturing phase.

In addition, the status of equipment auxiliary to the team's project should have been monitored from the beginning. The broken vacuum pump is an example of where this oversight

would have been helpful. Had more attention been paid to making sure the vacuum chamber was leak free and its pumps operational, it is possible that any problems could have been resolved in time.

The project met all the construction and writing requirements. However, due to unforeseen circumstances, namely the mechanical roughing pump on the vacuum chamber breaking, the apparatus was not being able to be tested. It is the belief of the team that upon repair of the vacuum chamber the assembly will be ready to mount and run immediately.

Works Cited

[1] Bennett, W., Ogunjobi, T., Menart, J. A., 2007, "Computational Study of the Effects of Cathode Placement, Electron Energy, and Magnetic Field Strength on the Confinement of Electrons." Paper #5248, AIAA-2007-5296, 43rd AIAA/ASME/SAE/ASEE Joint Propulsion Conference & Exhibit, Cincinnati, OH.

[2] Halliday, D., 2005, *Introduction Fundamentals of Physics*, John Wiley & Sons, Inc.

[3] Chen, F. F., 1984 *Introduction to Plasma Physics and Controlled Fusion Volume 1: Plasma Physics*, Plenum Press, New York and London.

[4] Fitzpatrick, R., 2006 *The Plasma Frequency.* University of Texas at Austin, http://farside.ph.utexas.edu/teaching/plasma/lectures/node6.html.

[5] Shukla, P. K., Mamun, A.A., 2001, *Introduction to Dusty Plasma Physics*, Institute of Plasma Physics Publishing, Bristol and Philadelphia.

[6] Lieberman, M. A., Lichtenberg, A. J., 1994, *Principles of Plasma Discharges and Materials Processing*. John Wiley & Sons, New York, New York.

[7] Jahn, R. G., 1968 *Physics of Electric Propulsion*. Dover Publications, Inc. Minola, New York.

[8] Bittencourt, J.A., 2004, *Fundamentals of Plasma Physics*. Pergamon Press. New York, New York.

[9] *Download Area for Poisson SuperFish,*
htttp://laacg1.lanl.gov/laacg/services/download_sf.phtml

[10] Moore, M.H., Davis, C.C., Coplan, M.A., 2003, *Building Scientific Apparatus*. Perseus Books. Cambridge, Massachusetts.